D8.8.3 REPORT ON THE IQMULUS PROCESSING CONTEST – YEAR 3

Deliverable D8.8.3

Circulation:	PU - Public
Lead partner:	CNR-IMATI-GE
Contributing partners:	CNR-IMATI-GE, TUDelft, FOMI
Authors:	Marco Attene (CNR-IMATI-GE); Silvia Biasotti (CNR-IMATI-GE); B.G.H. Gorte (TUDelft), Daniel Kristof and Angéla Olasz (FOMI)
Quality Controller:	Tor Dokken (SINTEF)
Version:	1.0
Date:	31.10.2015

Consisting of

SINTEF	STIFTELSEN SINTEF, Department of Applied Mathematics, Oslo, Norway
Fraunhofer	Fraunhofer Institute for Computer Graphics Research, Darmstadt, Germany
CNR-IMATI-GE	Institute for Applied Mathematics and Information Technologies of the National Research Council (CNR-IMATI), Genova, Italy
MOSS	M.O.S.S. Computer Grafik Systeme GmbH (MOSS), Munich, Germany
HRW	HR Wallingford Ltd (HRW), Wallingford, UK
FOMI	Hungarian National Mapping and Cadastral Agency (FÖMI), Institute of Geodesy, Cartography and Remote Sensing, Budapest, Hungary
UCL	University College London (UCL), Research centre for Photogrammetry, 3D Imaging and Metrology, London, UK
TUDelft	Delft University of Technology (TUDelft), Department of Earth and Climate Sciences & Man-Machine Interaction Group, Delft, The Netherlands
IGN	Institut National de l'Information Géographique et Forestière (IGN), Paris, France
UBO	Université de Bretagne Occidentale (UBO), European Institute for Marine Studies, Brest, France
Ifremer	L'Institut Francais de Recherche pour l´Exploitation de la Mer (Ifremer), Brest, France
Liguria	Regione Liguria, Genova, Italy

DOCUMENT HISTORY

Version[1]	Issue Date	Stage	Content and Changes
1.0	Oct 31 2015	Final	

[1] Integers correspond to submitted versions

EXECUTIVE SUMMARY

The deliverable D8.8.3 is related to the Third Year's activity of the IQmulus Task 8.5, described as follows in the Description of Work (DoW):

Focus of the task will be the dissemination of IQmulus results on data processing by means of setting up and running yearly contests, open to the whole scientific community as well as user groups, on research issues which are relevant to the WP4 area of work.

This report describes the process of selection of the most interesting tasks/services proposed as contest tracks and a description of the proposed challenges. In addition, we list the panel of experts, selected among the partners and involving scientists outside the consortium that have been chosen to support the planning of the contest, establish the processing tasks to be benchmarked and select the appropriate data set, performance measures and procedures to realize the validation. Finally, we add in the Appendix the guide to access the infrastructure hosted at IMATI and the reports of the three tracks presented during the ISPRS GeoBigData Workshop held in La Grande Motte (F), October 2nd, 2015.

Table of contents

1 INTRODUCTION

The IQmulus Processing Contest started in 2013 to provide the scientific community and practioners working in the field of 3D point cloud processing with certified benchmarks and ground truths in geospatial data processing. While in 2013 the tracks (and therefore the challenges to be approached) were proposed by partners involved in the WP4, in the second year calls for track proposals were specifically targeted to the project stakeholders. Once the tracks proposed have been validated and accepted by the Advisory Board, they have been publicized with specific call for participations and through a set of mailing lists (among the others the geometryprocessing list "geometryprocessing@inria.fr"). A similar procedure has been used for IQPC 2015 too, but a few significant changes have been introduced. Besides the usual "open" call for tracks, this year a limited number of personal invitations have been sent to scholars with an exceptional background in areas of particular interest for IQmulus. Furthermore, a "Best Track Award" has been established to acknowledge the organizers of the most successful track: the evaluation to assign the award is conducted by the Advisory Board based on the datasets proposed for each track, the ground truth, the accuracy and technical soundness of the evaluation methodology.

The results of the contests have been made publicly available and presented at the ISPRS GeoBigData Workshop held in La Grande Motte (F), October 2nd, 2015, where a special session on IQPC 2015 has been organized. The GeoBigData Workshop is part of the ISPRS GeoSpatial Week (La Grande Motte (France), September 28th - October 2nd, 2015). Participation to the contests is still possible thanks to a continuous submission procedure of executable codes or results; this is expected to make the participation in the contests more attractive for scientists.

This report describes the third year's activity of the IQmulus processing contest and describes the challenges faced by contest tracks. In addition, we list the panel of experts, selected among the partners and involving scientists outside the consortium that have been chosen to support the planning of the contest, establish the processing tasks to be benchmarked and select the appropriate dataset, performance measures and procedures to realize the validation.

1.1 ADVISORY AND TECHNICAL BOARDS

To allow a large scientific consensus, the IQmulus contest is implemented in collaboration with the research community and the support of an international advisory board, composed of high level scientific and technical experts in the field.

The composition of the Advisory Board for the third year is the same as for the second year. Specifically, the members of the IQmulus consortium involved in the Committee/ Advisory Board are:

- Silvia Biasotti, CNR-IMATI-GE
- Giuseppe Patanè, CNR-IMATI-GE
- Jan Boehm, UCL
- Nicolas Paparoditis, IGN
- Roderik Lindenbergh, TUDelft

The members of the Advisory Board that are external to the IQmulus project are:

- Hamish Carr, Visualization and Virtual Reality Group, University of Leeds, UK;

- Debra Laefer, School of Civil, Structural & Environmental Engineering, University College Dublin, Ireland. Debra Laefer is the recipient of the European ERC Starting Grant "RETURN: Rethinking Tunnelling in Urban Neighbourhoods", 2013-2017.

In addition, for the management of the third year's platform an IQPC'15 Technical Board has been established at IMATI-CNR, Italy. People involved in this activity are:

- Corrado Pizzi, IMATI-CNR, Italy
- Piero Bruno, IMATI-CNR, Italy
- Davide Sobrero, IMATI-CNR, Italy

2 TIMELINE OF THE CONTEST

In the following, we briefly summarize the different steps of the preparation of the third year IQmulus Processing contest.

10/10/2014 - Internal meeting at CNR-IMATI. This is the first action taken for IQPC 2015. The new task leader Marco Attene, together with Silvia Biasotti, Michela Spagnuolo and Bianca Falcidieno, all from IMATI, established a strategy to attract more track submissions.

13/10/2014 - First agreements with ISPRS representatives. Nicolas Paparoditis and Mathieu Bredif, who are chairs of Geospatial Week 2015 and the GeoBigData workshop respectively, were contacted to agree on the organization of a special session of IQPC 2015 as part of the workshop.

12/11/2014 - Agreements for the publication of track reports. GeoBigData organizers confirm that IQPC reports can be submitted as scientific papers to appear in the ISPRS Archives of the Photogrammetry, Remote Sensing and Spatial Information Sciences.

15/12/2014: Call for tracks and personal invitations circulated. The first call for tracks has been published and circulated throughout the same channels used in 2013 and 2014. Also, this year a limited number of personal invitations have been sent to scholars with an exceptional background in areas of particular interest for IQmulus.

20/01/2015: Track proposals due. Potential track organizers submit their proposals as a text document containing: proposed processing task and its relevance; datasets to be used for the evaluation; ground truth, if applicable; criteria envisaged to evaluate the codes; evaluation methodology; expected number of participants; envisaged dissemination channels for advertising the track (material was sent to marco.attene@ge.imati.cnr.it as specified in the call)

02/02/2015 - First IQPC Website published. The first version of IQPC 2015 Website has been published at http://www.ge.imati.cnr.it/?q=node/262. Track titles and organizers are reported on this Website. Another Web-page with the same contents has been published in the IQmulus official Website at http://iqmulus.eu/iqpc/iqmulus-processing-contest-2015 .

03/02/2015: Guide to access the CPU-cluster infrastruction circulated. All the track organizers received the document and access rights to exploit the cluster for running the contests.

15/04/2015: Abstracts of track reports submitted. Each track submitted an extended abstract to ISPRS GeoBigData Workshop. These reports include the description of the track, the datasets and the evaluation methodology, but not the actual results of the experimentation.

01/07/2015: Full reports submitted. Each track submitted a full paper to ISPRS GeoBigData Workshop, as an extension of the previously submitted abstract. These papers describe the track in all the details, and include the actual results of the experimentation.

02/10/2015: Oral presentation of the tracks. The IQPC special session concludes the Geo-BigData workshop, and Best Track Award has been assigned to Dr. Linh Truong-Hong (Figure 1) and Prof. Debra Laefer (both from University College Dublin, Ireland) for the organization of the track on EVALUATION OF AUTOMATICALLY GENERATED 2D FOOTPRINTS FROM URBAN LIDAR DATA.

FIGURE 1: DR. TRUONG-HONG ANSWERS A QUESTION FROM THE AUDIENCE

3 THE CONTEST INFRASTRUCTURE

As detailed in the deliverable 8.8.1, the IQmulus Processing contest is hosted in a CPU-cluster unit installed at IMATI-CNR. The processing and storage capabilities of the original IQmulus cluster have been increased by an additional node hosting the Visualisation Virtual Services (VVS) offered by the FP7-INFRASTRUCTURES project VISIONAIR (2011-2015).

In 2014 track organizers and participants could exploit the infrastructure through the Collage Authoring Workbench, http://collage.ge.imati.cnr.it. However, for 2015 we have decided to let the track organizers and the participants access the CPU-cluster directly through an SSH connection, as described in Appendinx 0.

3.1 MULTI-PLATFORM CLUSTER

CNR-IMATI provides a multi-platform infrastructure including five virtual machines, each of them hosting a different operative system and providing different hardware settings, described in the table below:

LINUX	WINDOWS
UBUNTU1 ➢ **Operative System:** Ubuntu 12.04 64bit ➢ **Processors:** 8 ➢ **RAM:** 16 GB ➢ **IP Address:** 172.16.10.31 **UBUNTU2** ➢ **Operative System:** Ubuntu 12.04 64bit ➢ **Processors:** 8 ➢ **RAM:** 16 GB ➢ **IP Address:** 172.16.10.32 **UBUNTU3** ➢ **Operative System:** Ubuntu 12.04 64bit ➢ **Processors:** 8 ➢ **RAM:** 16 GB ➢ **IP Address:** 172.16.10.33	**WINDOWS2-32** ➢ **Operative System:** Windows7 32bit ➢ **Processors:** 8 ➢ **RAM:** 3 GB ➢ **IP Address:** 172.16.10.34 **WINDOWS1-64** ➢ **Operative System:** Windows7 64 bit ➢ **Processors:** 8 ➢ **RAM:** 16 GB ➢ **IP Address:** 172.16.10.35

Each virtual machine provides also some software tools, IDEs and libraries compatible with the underlying operative system.

All the Ubuntu-like machines are equipped with:

- GCC Compiler 4.6
- Octave Packages 3.2.4 (MATLAB-like)
- Wine 1.4
- PCL Library 1.6 and 1.7
- GDAL 1.7.0

In case a participant has a specific request (particular operative systems, 32bit versions of the operative systems and/or someone needs a particular virtual machine) CNR-IMATI foresaw the possibility of providing ad-hoc virtual machines. Participants may also provide to CNR-IMATI their own virtual machine, properly set to run their executables.

Credentials to access to the infrastructure are provided upon request to the track organizers to run the executables the participants submitted them. Instructions to access the infrastructure (attached in the Appendix) have been distributed to the track organizers.

4 THE THIRD YEAR'S TRACKS

The contest enables reproducible evaluation through the creation of standardized benchmarks and evaluation methodologies. In the third year, three track proposals have been selected as representatives of acute issues in geospatial data: i) Evaluation of automatically generated 2D footprints from urban Lidar data ii) Water detection and classification on multisource remote sensing and terrain data and iii) Tree separation and classification in mobile mapping Lidar data.

In the remainder, a summarizing description of the three tracks implemented in 2015 is given. Further details can be found in each Track's specific website and in the Appendix of this document, where we attach the reports of the contest contributions presented at the ISPRS GeoBigData Workshop.

4.1 EVALUATION OF AUTOMATICALLY GENERATED 2D FOOTPRINTS FROM URBAN LIDAR DATA

The description of the track is hosted at the address: https://sites.google.com/site/iqpc15/ and has been proposed by Dr. Linh Truong-Hong, University College Dublin, Ireland and Prof. Debra Laefer, University College Dublin, Ireland (linh.truonghong@ucd.ie, debra.laefer@ucd.ie).

At the time of the presentation at the GeoBigData Workshop (October 2nd, 2015), one participant applied to this track.

Objectives

The goal of this track is to evaluate the 2D footprints of a city scale automatically from ALS data. The participants are asked to submit the results of automatically generated 2D building footprints (Task A) and/or 2D road profiles (Task B) from three pre-designated sections of the 1 km^2 study area. The contest organizers evaluate submitted results based on the ground truth derived from both Ordinate Survey Ireland (OSI) and OpenStreetMap. A winner and two runners up for each task are selected based on the overall evaluation score.

Task A is to extract a point cloud affiliated with buildings and to reconstruct 2D building footprint from these points. Participants are asked to submit two sets of file results: (1) ASCII files containing ALS data sets of each building, where each row represents the x-, y-, and z-coordinates of the data points, and (2) ASCII files containing the building footprint as a polygon, where each row contains both the x- and y- coordinates of the polygon vertices. The file naming convention should be "Building_X1_Y1_X2_Y2", where the pairs X1and Y1 and X2 and Y2 are two opposite corners of the bounding box of the dataset on a horizontal plane.

Task B is to extract a point cloud of the roads and to reconstruct 2D road profiles including the pavement edges. Similar to Task A, the participants are asked to submit two ASCII files containing: (1) ALS data points of the road network and (2) the polygons describing pavement edges of the road network. In the case that only ASCII files containing data points of either buildings or road network are submitted, the building footprints and the pavement edges of the road are generated by the organizer's algorithm for further evaluation.

Data Description

The test area is approximately 1 km^2 and consists of 205 blocks, each of which may contain in excess of a dozen buildings per block, as shown in Figure 1. The typical building is 11–15m in height, less than 5m in width, and 6–10m in length. The buildings are mostly closely spaced or

abutting each other, with some sharing an adjoining wall, commonly referred to as a “party wall”.

The dataset was acquired by ALS using the FLI-MAP 2 system, which generated 1000 pulses for each scan line. The system operated at a scan angle of 60 degrees. The quoted accuracy of the FLI-MAP 2 system is 8 cm in the horizontal plane and 5cm in the vertical direction, including both laser range and navigational error. Acquired points were provided in a global coordinate system with reference to the National Irish Grid (Irish Grid), relating to the use of a Global Navigation Satellite System (GNSS) to determine the aircraft position during scanning. The FLI-MAP 2 system is capable of recording up to four echoes for each emitted pulse and spectral data with intensity values.

The dominant directions of the flight tracks were chosen as north-east, north-west, south-east and south-west. The flight attitude varied between ~380-480m (as low as possible with respect to approval by the Irish Aviation Authority), with an average elevation of ~400m. A total of 44 flight strips with 2,823 flight path points were collected during data acquisition. As a result, a point cloud was merged from 370,154 scan lines with approximately 225 million data points in total. Each emitted pulse was recorded with up to four echoes. The echo distribution is shown in The vast majority of points were first echoes. Secondary echoes constituted only a small portion of the points, as the overwhelming majority of surfaces in the study area were solid objects, in the form of streets and buildings. For further information about this ALS data, participants are referred to the following reference. The data set was organized into 9 tiles, each covering 500m x 500m (Figure 1).

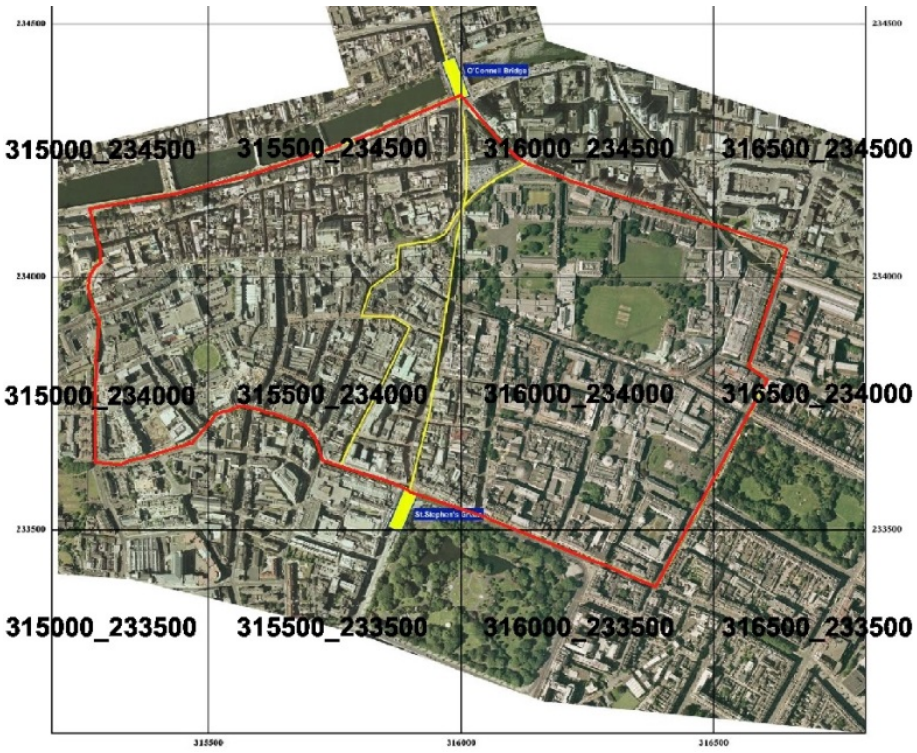

FIGURE 2: ACQUIRED ALS AREA IN DUBLIN CENTRAL AND ALS TILES (CONTEST AREA OUTLINED IN RED)

Three subsets of the data are used for this competition (Figure 2). Area 1 contains sparse buildings, larger green area, and trees. Area 2 has both building blocks and buildings sharing walls, as well as separate trees. Area 3 contains low brick buildings and no trees.

The data set of entire study area is organized in 9 files, each representing a 500m x 500m tile. The 5.8 Gb of data have an LAS extension.

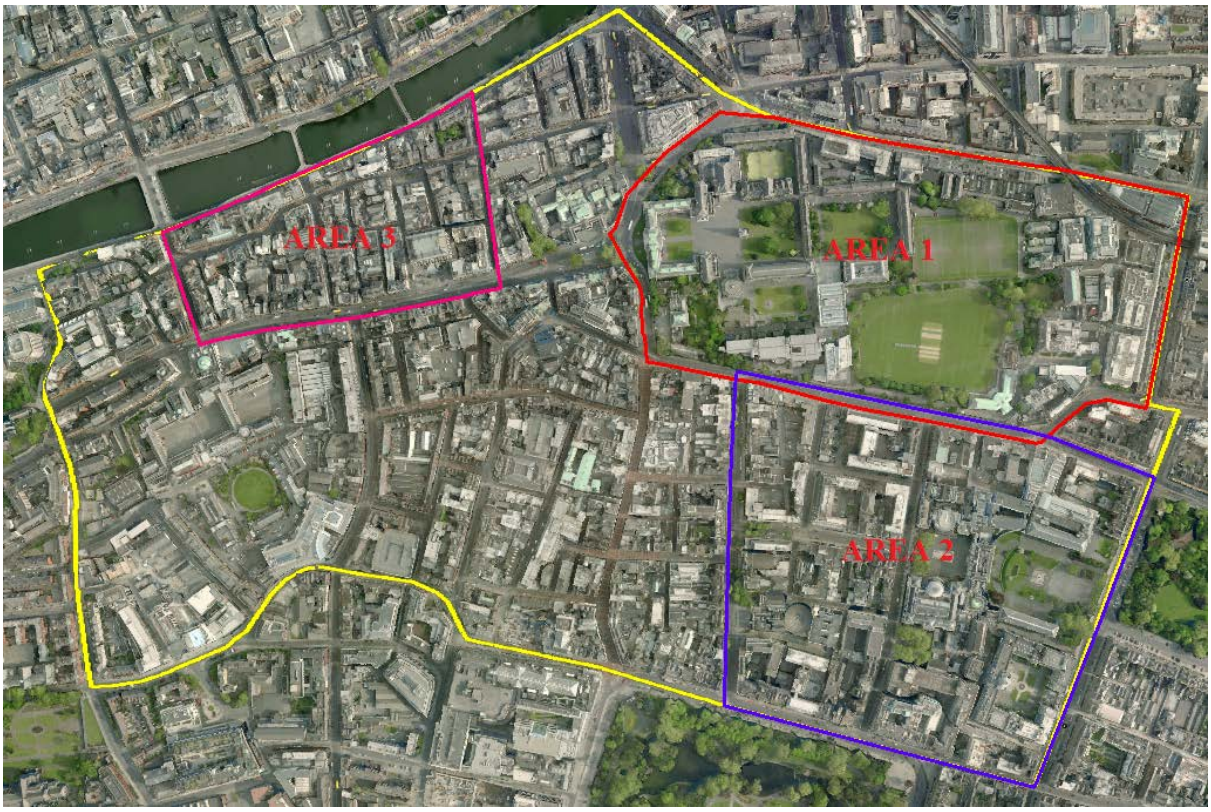

FIGURE 3: CONTEST AREAS

The "ground truth" is a set of 2D footprints provided by the OSI. The 2D footprints primarily consist of 2D building boundaries and road profiles (centre and edges). However, as buildings and road network can be changed over period time, the building boundaries and road centre derived from OSM were used as complement resource (Figure 3).

FIGURE 4: GROUND TRUTH FROM OSI AND OSM

Evaluation

Task A **-** The evaluation process identifies the level of locational deviation, the level of shape similarity, and the positional accuracy of the extracted building footprint (ExB), with respect to the ground truth building (GtB). For the location deviation, quality indicators involving True Positive (TP), False Positive(FP) and False Negative (FN) is used to measure the overall extraction and reconstruction of the building footprints. These indicators can be determined after mapping extracted results onto the GtB. If the object from the ExB matches one from the GtB, it is TP. If the object from ExB does not match to one from the GtB, it is FP; otherwise, if

the object from GtB does not match one from the ExB, it is FN. These quality indicators are illustrated below. Completeness, correctness, and quality are the measured indicators of the submitted results (details in Appendix).

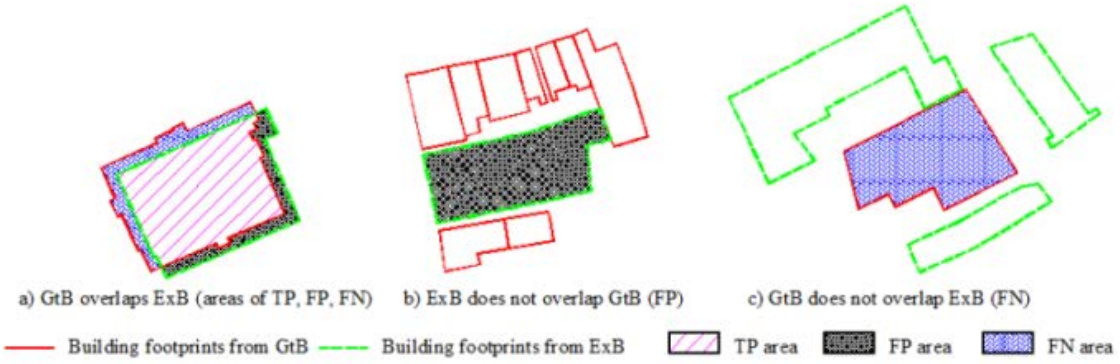

FIGURE 5: ILLUSTRATION OF DETERMINING TP, FP, AND FN

Task B - The evaluation process also identifies the level of locational deviation and the positional accuracy of the extracted road profile (*ExR*) with respect to the ground truth road (*GtR*). Based on the minimum bounding box of *GtR*, a 2D grid with the cell size of 1m x 1m is generated. When the *GtR* is mapped onto the 2D grid, the cell, $C_{GtRi}(x,y)$, has a value of 1, if any pavement edge of the *GtR* overlaps the cell (green cells in a figure below); otherwise the value of $C_{GtRi}(x,y)$ is 0 (white cells in a figure below). Furthermore, the cell with $C_{GtRi}(x,y) = 1$ is divided into two parts called inside road ($C_{GtRInti}(x,y)$) and outside road ($C_{GtROuti}(x,y)$, where $C_{GtRInti}(x,y)$ is a part of the cell having the centre drops between two pavement edges of the road; otherwise it is $C_{GtROuti}(x,y)$. Notably, a total area of $_{CGtRInti}(x,y)$ and $C_{GtROuti}(x,y)$ equals to the cell area = $1m^2$. This rule is also applied for *ExR* when projecting *ExR* onto the 2D grid.

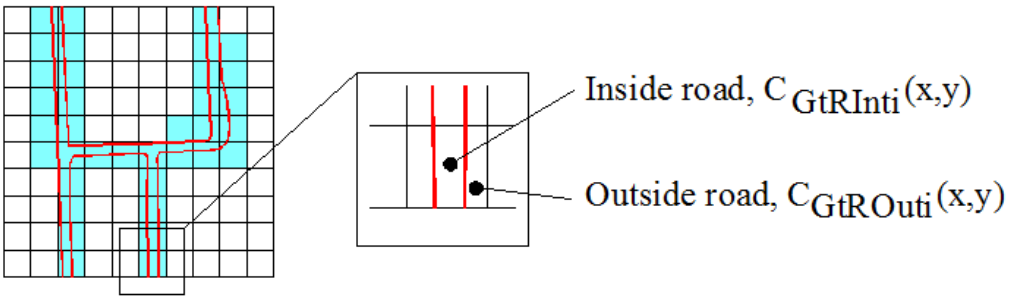

FIGURE 6: CLASSIFICATION OF CELLS IN 2D GRID: GREEN CELLS = 1, WHITE CELLS = 0

The location deviation, completeness, correctness, and quality indicators mentioned in Task A are measured, where these parameters can be determined from Eq.1-3. True Positive (*TP*), False Positive (*FP*) and False Negative (*FN*) are computed by comparing cell values from two 2D grids represented by *GtR* and *ExR* (details and equations in Appendix).

4.2 WATER DETECTION AND CLASSIFICATION ON MULTISOURCE REMOTE SENSING AND TERRAIN DATA

The description of the track is hosted at the address: http://iqmulus.eu/iqmulus-processing-contest-2015/2-water-detection-and-classification-on-multi-source-remote-sensing-and-terrain-data. It has been organized by FÖMI, Institute of Geodesy, Cartography and Remote

Sensing, 1149 Budapest, Hungary (A. Olasz, D. Kristóf, M. Belényesi, K. Bakos) and D. Kristóf (kristof.daniel@fomi.hu) is the contact person.

At the time of the presentation at the GeoBigData Workshop (October 2nd, 2015), one participant applied to this track.

This processing track addresses a particular problem in the field of big data processing and management with the objective of simulating a realistic remote sensing application scenario. The main focus is on the detection of water surfaces (natural waters, flood, inland excess water, other water-affected categories) using remotely sensed data. Multiple independent data sources are available and different tools could be used for data processing and evaluation. The main challenge is to identify the right combination of data and methods to solve the problem in the most efficient way.

The first task is to determine the most useful input source and the processing methodology most useful for the problem. In real-life situations a careful optimization is needed in order to not only obtain the best possible achievements in terms of processing accuracy, but also from the resource and time efficiency viewpoints. In generic terms, one has to evaluate the available inputs and processing methodologies and to select an optimum solution that can fit into the available time frame with the available resources (computing, human). In this track a challenge is defined to address the problem of detecting water surfaces and different categories of water-affected soils and vegetation, covered by a variety of remotely sensed data of multiple resolutions.

Objectives

The goal of this track is **to detect water-related thematic classes** in a specific area in Hungary.

The track leader provides a wide array of remote sensing data covering the area in concern, including:

- high-resolution aerial hyperspectral imagery,
- high-resolution visible (RGB) orthophotos,
- Terrain model (DTM) and surface model (DSM) derived from airborne LiDAR point clouds,
- medium-resolution (Landsat 8) satellite imagery

The participants have to provide thematic maps with a set of pre-defined categories. A set of calibration and validation samples are provided to train and validate the various processing chains, and final evaluation are carried out by the track leader using independent samples.

Competitive solutions have to fulfil the following criteria:

- Create the best possible classification using the simplest set/combination of input sources
- Try to reduce the number of input data for the processing
- Develop algorithms that are fast to run
- Find the best balance of complexity and accuracy (maximize efficiency) during the data processing

The study area is divided into three parts:

- Area A: the full study area with medium-resolution Landsat 8 coverage

- Areas B and C: two sub-areas with full high-resolution data coverage.

The participants have to provide thematic maps for each of the areas (A, B and C) with the below categories:

- Water surfaces (code: 1)
- Wet/waterlogged soils (code: 2)
- Soils not directly affected by water (code: 3)
- Vegetation standing in water (code: 4)
- Vegetation not directly affected by water (code: 5)
- Other (code: 0)

For each area, a set of training and verification samples are provided by the track leader in vector format, covering each of the above thematic categories. The participants can use the samples to train the classification algorithms and to verify the results. Areas with both high- and low-resolution data coverage (B and C) can be used to tune the algorithms for better performance on the larger area with only Landsat data (area A).

Participants have to submit the following material:

- Georeferenced thematic rasters in GeoTIFF format, containing the codes of thematic categories as described above
- Concise description of the whole methodology and processing chain (including algorithms and parameters, with references to relevant literature wherever available)

Data description

Location: The input datasets cover a study area in Hungary (Figure 6). The area of interest is on the North-East part of the country along the river Bodrog. The lowest point of the area is on 77, 19 m above the sea level, the highest point is on 258,73 m above the sea level.

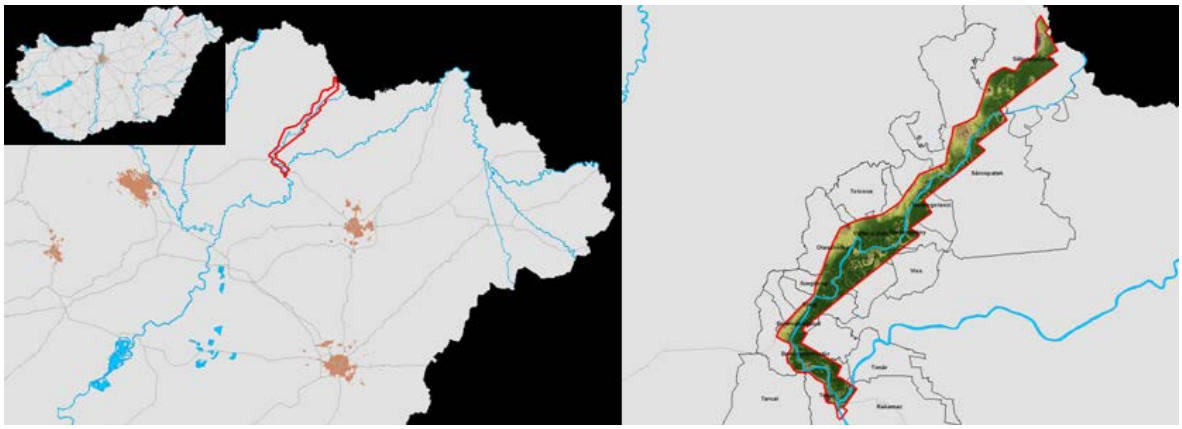

FIGURE 7: LOCATION OF THE DATASET

Landsat 8 data is provided for the whole area A, whereas hyperspectral images, LiDAR-derived Digital Surface (DSM) and Terrain Model (DTM) and orthophotos (RGB) are additionally provided for areas B and C (Figure 7).

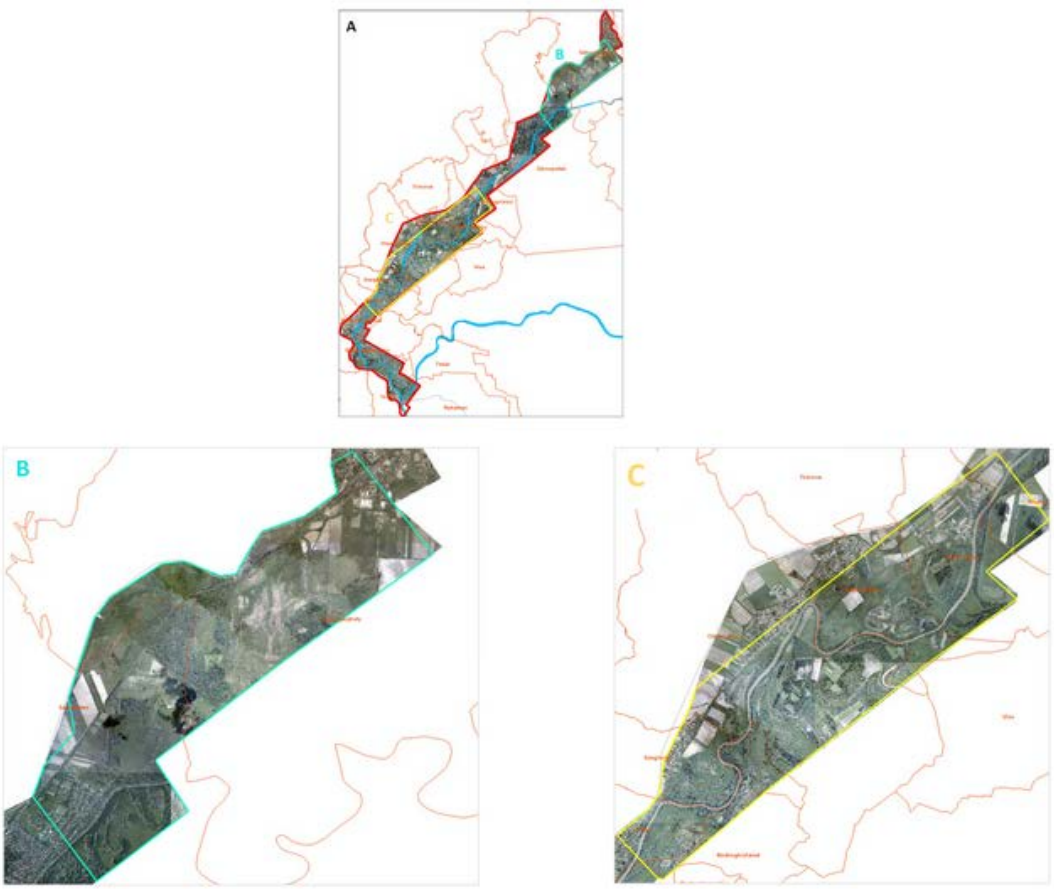

FIGURE 8: AREAS OF THE DATASET

Evaluation

The evaluation and scoring are developed based upon the complexity, time- and resource efficiency of the methodology and the data requirement for processing. This means that the best result is the simplest solution that is fast and easy to carry out, requires less input, however it is accurate enough to address the problem.

The track leader assesses the results submitted by each participant by using a verification sample set independent of those provided to the participants.

4.3 TREE SEPARATION AND CLASSIFICATION IN MOBILE MAPPING LIDAR DATA

The description of the track is hosted at the address: http://homepage.tudelft.nl/41s94/iqmulus/Contest3.html and has been proposed by Ben Gorte, Delft University of Technology, The Netherlands (B.G.H.Gorte@tudelft.nl).

At the time of the presentation at the GeoBigData Workshop (October 2nd, 2015), three participants applied to this track.

Objective

The goal of this Track is to establish the state-of-the-art of available algorithms for detection of individual trees in point clouds. The focus is on point clouds obtained by Mobile Mapping

Systems (MMS), and therefore on trees that are in the vicinity of the public road network, notably in urban environments.

Analysis of laser-generated point clouds for forest applications has already gained a good reputation. For the purpose of forest inventories, for example, laser data are being analysed to estimate the number of trees in a forest, identify species, and estimate wood volumes. For large forest areas, airborne laser scanning is the preferred data source, whereas for detailed studies at individual tree level also terrestrial laser scanning is being used.

This Track concerns point clouds obtained by mobile mapping systems (MMS). Such systems typically integrate laser scanners, cameras and navigation sensors (GPS, IMU and odometers). They are mounted on cars or trucks and capture data while driving. Initiatives from various agencies and companies using different MMS equipment are currently being excuted and will eventually capture the entire road network with the surrounding objects.

At the same time there is an interest of municipalities and other authorities to form databases ("cadasters") of the trees in the public space they manage. Many trees are located along streets and roads, and are therefore capture in MMS campaigns. In order to record information at the individual tree level, it is necessary to identify those individual trees in the data. This issue is, for example, addressed at boomregister.nl for the entire Netherlands.

By visual inspection of MMS point clouds it is possible to do the tree identification manually, but this is obviously time consuming. The processing contest, therefore, addresses automation of this task. Two sub-tasks can be easily identified:

1. Classifying the points of an MMS pointcloud into two classes: tree points and other points
2. Separating the tree points in a point cloud into the individual trees

The emphasis in this contest is on separation. Therefore, the primary task for participants in the contest is to separate the trees in a given point cloud that contains only tree points.

In addition, participants are invited to analyse the raw MMS data, from which the tree points were extracted. The provided tree points only represent a subset of about 30 trees, but actually the number of trees in the area is much larger. Therefore, participants who have access to classification software are challenged to identify as many tree points as possible, in addition to the ones provided, and after that separate the entire set of tree points into individual trees.

Data Description

The MMS dataset is located at the campus of TU Delft in the Netherlands. It is obtained by the Fugro DRIVE-MAP system (Figure 8). Fugro organizes the data in tiles of 25x25m. The raw data consists of no less than 509 tiles, therefore occupying an area of about 318,000 m^2. Note that many tiles contain only very few points, and serve to fill up gaps between the other tiles (that do contain a lot of points). The total number of points is about 60 million.

FIGURE 9: THE FUGRO DRIVE-MAP SYSTEM

Some 30 large trees were selected in a part of the area, which is contained in 26 tiles. There are some 10 million points in those 26 tiles, and the selected trees are made up of 1.8 million points.

The challenge of the contest is therefore:

1. to subdivide dataset 1 or dataset 2 into as many groups as there are trees (approximately 30), and label the points accordingly.
2. to classify (re-label) *unclassified* points in dataset 3, or in the combined datasets 3 and 4, as tree points where appropriate, and subdivide the entire set of tree points (the given ones and the newly classified ones) by labelling the points with unique tree numbers.

Evaluation

The evaluation of challenge 1 is quantitave on the basis of the number of correctly labeled trees, and qualitive, by visual inspection, on how well the points are assigned to the correct trees. The result gives the initial ranking of participants. In case of a draw, challenge 2 is considered. The criteria there are largely qualitive, by visual comparison of the results with the situation in the field.

5 FUTURE PLANS

The set up and the yearly run of open contests are crucial for the dissemination of the IQmulus results on data processing to the whole scientific community and user groups. The IQmulus Processing contest tracks have been presented during the ISPRS GeoBigData Workshop and the track reports (see the Appendix) have been published within ISPRS Archives of the Photogrammetry, Remote Sensing and Spatial Information Sciences. Two of the best papers presented to GeoBigdata'2015 will be selected and the authors will have the possibility to submit an extended version of their articles for review and possible publication on the ISPRS Journal of Photogrammetry and Remote Sensing.

Thanks to the feedback received from the members of the Advisory Board and the participants of the tracks of the first two IQmulus contests, new challenges are planned for the next editions of the contest, among others we list:

- Feature detection: extraction of significant shape characteristics (either geometric or semantic);
- Change detection, which is an acute issue in geospatial data and related to the task 4.5 of the IQmulus project.

For the next year we plan to strengthen the link with the panels of experts leaving the coordination of some tracks to members of the Advisory Board. In addition, we plan to increase the number of members of the Advisory Board.

Finally, similarly to IQPC 2014, we are planning to organize another IQmulus workshop with a special session dedicated to the Processing Contest. This important event will be part of the International Geometry Summit 2016 (http://www.geometrysummit.org/), which will be held in Berlin in June 20-24, 2016. The Geometry Summit puts together three of the most important conferences in areas such as geometric modelling and processing, and is therefore a significant opportunity to disseminate IQmulus results, thus including the Processing Contest, to a large and relevant audience.

6 CHANGE OF THE TASK LEADER

Since October 15, 2015 the leadership of the task is taken by Dr. Silvia Biasotti (CNR-IMATI).

7 APPENDIX

The Appendix contains a guide to access the CPU-cluster unit hosted at IMATI-CNR, and the three reports of the tracks presented at the ISPRS GeoBigData Workshop held in La Grande Motte (F), October 2nd, 2015 in co-location with the ISPRS GeoSpatial Week. Specifically, the remainder of this appendix is made of the following documents:

- Guide to Access the infrastructure
- Report on Track #1: Evaluation of automatically generated 2D footprints from urban Lidar data
- Report on Track #2: Water detection and classification on multisource remote sensing and terrain data
- Report on Track #3: Tree separation and classification in mobile mapping Lidar data

7.1 GUIDE TO ACCESS THE INFRASTRUCTURE

IQPC2015: CNR-IMATI Cluster

1. Cluster Infrastructure

CNR-IMATI provides a multi-platform infrastructure including five virtual machines, each of them hosting a different operative system and providing different hardware settings, described in the table below:

Linux	Windows
Ubuntu1 ➢ **Operative System:** Ubuntu 12.04 64bit ➢ **Processors:** 8 ➢ **RAM:** 16 GB ➢ **IP Address:** 172.16.10.31	**Windows2-32** ➢ **Operative System:** Windows7 32bit ➢ **Processors:** 8 ➢ **RAM:** 3 GB ➢ **IP Address:** 172.16.10.34
Ubuntu2 ➢ **Operative System:** Ubuntu 12.04 64bit ➢ **Processors:** 8 ➢ **RAM:** 16 GB ➢ **IP Address:** 172.16.10.32	**Windows1-64** ➢ **Operative System:** Windows7 64 bit ➢ **Processors:** 8 ➢ **RAM:** 16 GB ➢ **IP Address:** 172.16.10.35
Ubuntu3 ➢ **Operative System:** Ubuntu 12.04 64bit ➢ **Processors:** 8 ➢ **RAM:** 16 GB ➢ **IP Address:** 172.16.10.33	

Each virtual machine provides also some software tools, IDEs and libraries compatible with the underlying operative system.

All the Ubuntu-like machines are equipped with:

- GCC Compiler 4.6
- Octave Packages 3.2.4 (MATLAB-like)
- Wine 1.4
- PCL Library 1.6 and 1.7
- GDAL 1.7.0

In case participant has any specific request (particular operative systems, 32bit versions of the operative systems and/or someone need a particular virtual machine) CNR-IMATI foresaw the possibility of providing ad-hoc virtual machines. Participants may also provide to CNR-IMATI their own virtual machine, properly set to run their executables.

Credentials to access to the infrastructure are provided upon request to the track organizers to run the executables the participants submitted them.

2. Cluster Access Guide

The multi-platform infrastructure is available via SSH protocol. Participants must perform two SSH requests to access to the physical machine where the virtual machines are hosted and accessible through VCNViewer. Instructions to access a provided virtual machine from any operative system are provided below.

Note that VNCViewer is not a multi-user tool and does not allow several users to simultaneously access the system. Please, give up in using the system if you notice that someone else is taking advantage of the graphical user interface (eg. the graphical user interface provided by VNCViewer shows the mouse cursor moving, …) .

NB. No usernames neither passwords are provided in this guide. In the following instructions,

- `[GlobalUser]` must be replaced by the provided global username
- `[GlobalPw]` must be replaces by the provided global password
- `[PrivateUser]` must be replaced by the provided private username
- `[PrivatePw]` must be replaced by the provided private password

From Mac OSX

X11 is required to access the CNR-IMATI Cluster from Mac OSX platforms. If X11 is not included with your OS X, please install it before starting. Then:

1. Enable X11 Forwarding with the "X11Forwarding yes" option set in `/private/etc/sshd_config` for your SSH daemon's own local X11 host.
2. Restart sshd on the Mac OSX host from System Preference/Sharing pane on Mac OS X.
3. Perform the same operations described below for Linux /Mac OSX systems.

From Linux /Mac OSX

From any terminal, perform SSH accesses and start VNCViewer by using the following command lines:

1. SSH Access `ssh -C -X [GlobalUser]@150.145.8.226`
2. Password `[GlobalPw]`
3. SSH Access `ssh -C -X [GlobalUser]@172.16.10.11`
4. Password `[GlobalPw]`
5. VNCViewer `vncviewer localhost :1`
6. Password `[GlobalPw]`

From Windows

Some tools are necessary to access the CNR-IMATI Cluster from Windows platforms. Please, download the following required software before starting:

- Putty http://www.chiark.greenend.org.uk/~sgtatham/putty/download.html
- Real VNCViewer http://www.realvnc.com/download/viewer/

Then:

1. Open Putty 

2. From the Home Interface (Figure 1), set the following parameters:
   - Host Name (or IP Address): 150.145.8.226
   - Port: 22
   - Saved Sessions: IQPC2015
3. From the Tunnel Interface (Figure 2), set the following parameters:
   - Source Port: 12345
   - Destination: localhost:5901

   and press the “Add” button.
4. Go back to the Home Settings interface (from “Session” link on the left) and press the “Save” button.
5. Press the “Open” button to perform the first SSH access.

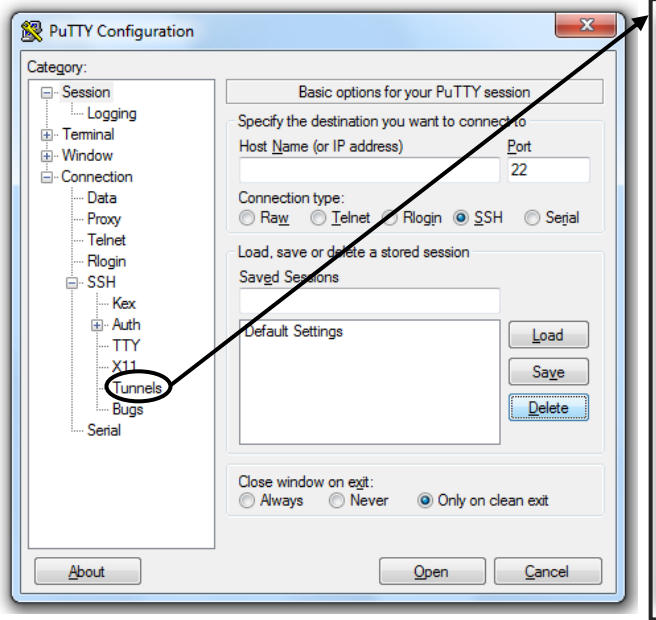

Figure 1: Putty - Home Settings

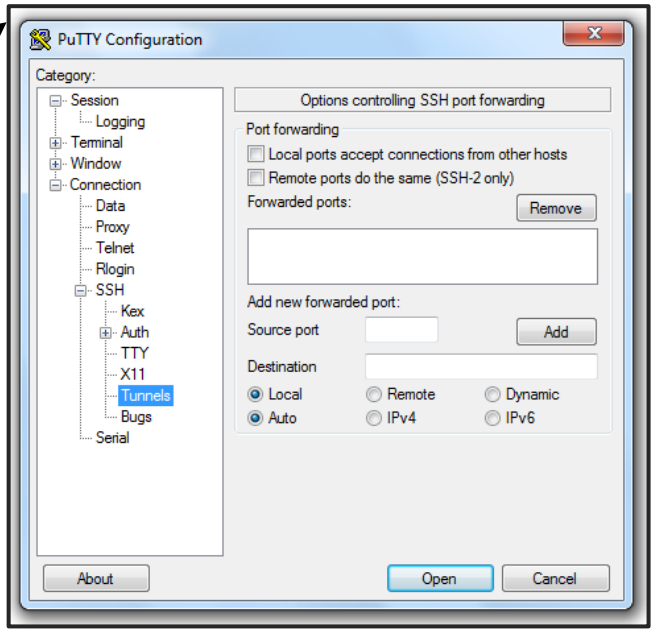

Figure 2: Putty - Tunnels Settings

6. From the putty command prompt, login by using the following credentials:
   - Username: `[GlobalUser]`
   - Password: `[GlobalPw]`
7. Leave the command prompt open and open VNCViewer 

8. From the VNCViewer interface (Figure 3), set the VNC Server to **localhost:12345** and press the "Connect" button.

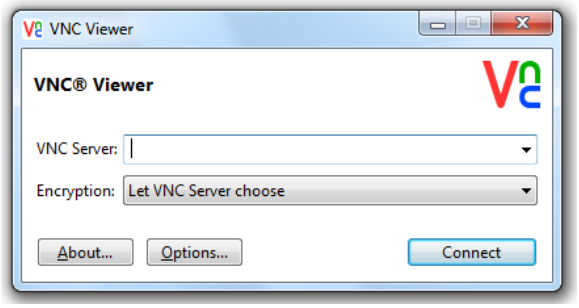

Figure 3: VNCViewer Interface

9. Enter the `[GlobalPw]` password.
10. The VNCViewer graphical interface will show the GUI of the system. If the system is in stand by and password is asked, enter the `[GlobalPw]` password.
11. From the menu bar at the top of the interface, select **Applications** → **System Tools** → **Terminal**.
12. From the terminal, perform SSH access and open VNCViewer by using the following command lines:
    1. SSH Access `ssh -C -X [GlobalUser]@172.16.10.11`
    2. Password `[GlobalPw]`
    3. VNCViewer `vncviewer localhost :1`
    4. Password `[GlobalPw]`

3. How to run a specific virtual machine

Once you are connected to the CNR-IMATI Cluster, the graphical user interface (Figure 4) allows you to run any available virtual machine. To access any virtual machine:

1. Select from the menu bar at the top of the interface **Applications → System Tools → Oracle VM VirtualBox.** The list of available virtual machines and their current state is shown (Figure 5).

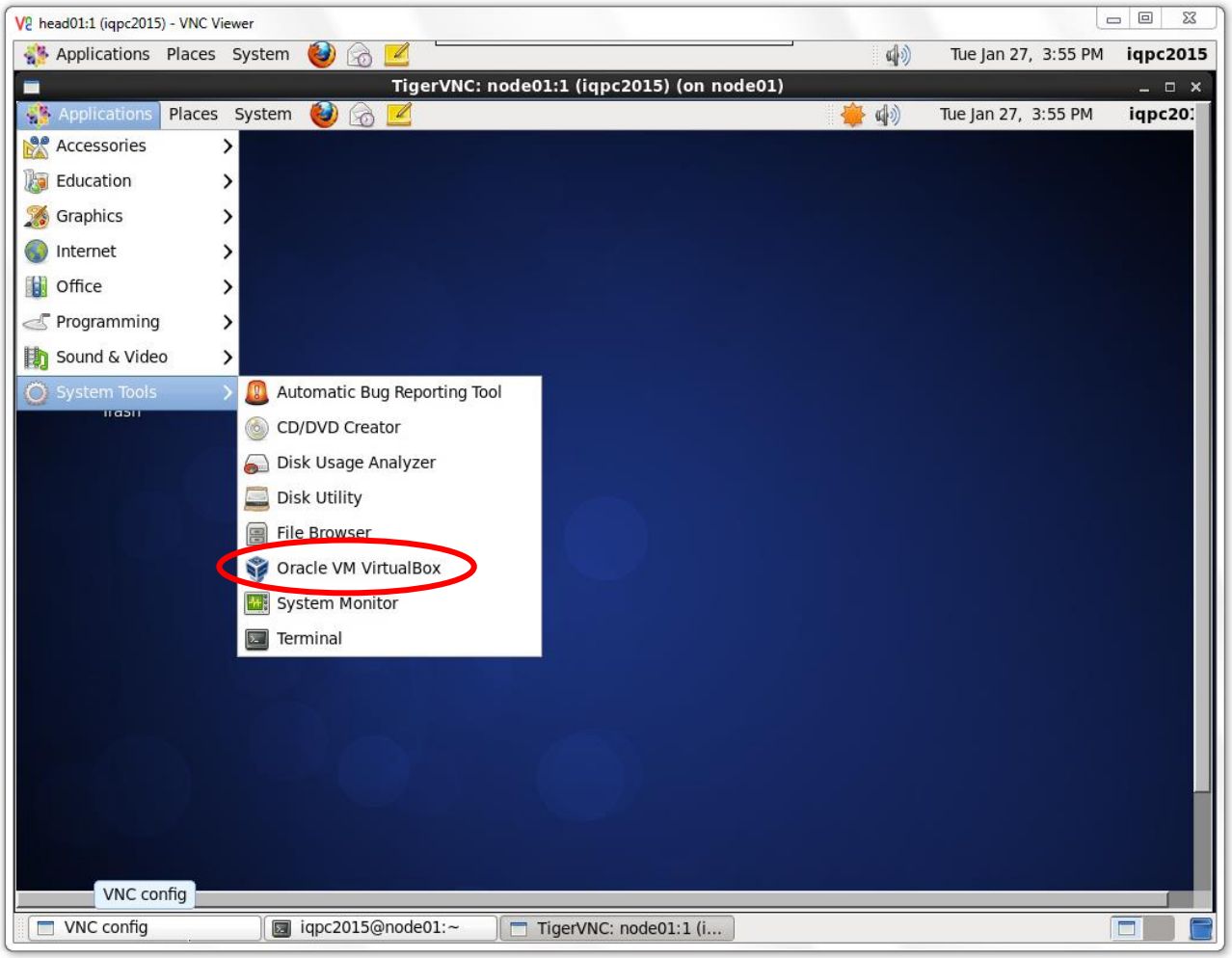

Figure 4: Cluster Graphical User Interface

2. Double click on the desired virtual machine, wait for starting the corresponding operative system, select the username assigned to you (`[PrivateUser]`) and enter your private password `[PrivatePw]`.

NB.1. Keyboard language is not set automatically in the virtualized systems. If you have any problem in typing special characters, please set the keyboard language manually from the operative system settings after you login.

NB.2. Systems are set to go into stand by after some inactive time. If it happens, the user will be asked to enter the `[GlobalPw]` password twice.

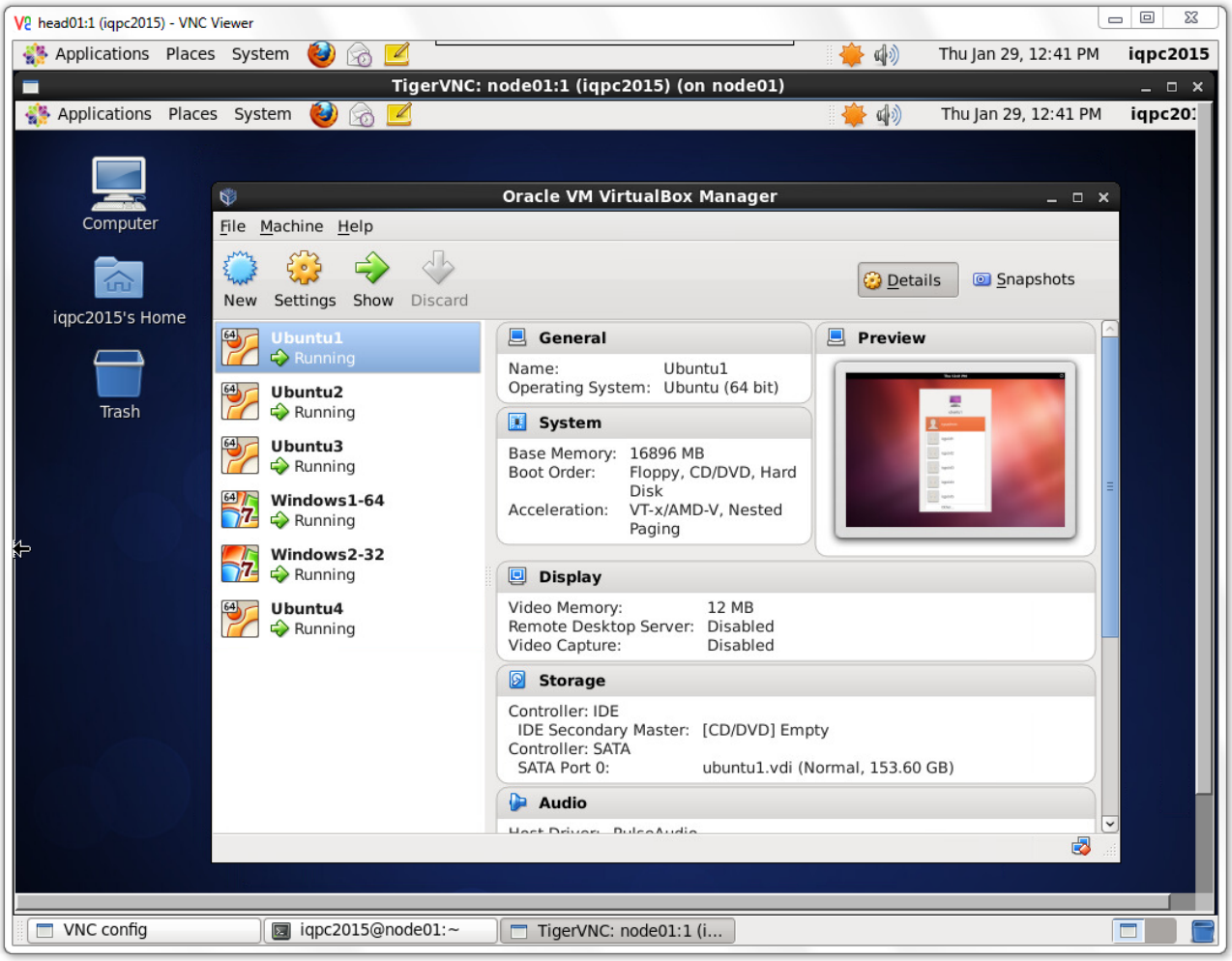

Figure 5: Cluster Graphical User Interface – Available Virtual Machines

In order to assure that all the available resources are dedicated to run your experiment, only a single virtual machine should be running at that moment. All the others should be powered off. Please, run the virtual machine you are intending to use and power it off when you have finished with you experiments. To power the running virtual machine off, you can simply switch off the corresponding operative system or right click the running virtual machine from the VM VirtualBox Manager (Figure 5) and select the **Close → Power Off** option.

4. How to transfer data from local machine to virtual machine

The transfer of data from your local machine to a selected virtual machine requires three steps. Modalities to perform each step are explained below, based on the operative systems installed both on your local machine and on the selected virtual machine.

In the following instructions,

- `[UserFile]` indicates the global path of the file or directory on the user machine
- `[ClusterFile]` indicates the relative path of the copied file or directory on the cluster
- `[VMFile]` indicates the relative path of the copied file or directory on the selected virtual machine

NB.1. You are allowed to copy files and directories only to your assigned account, that means that `[ClusterFile]` should be any path starting from `/home/[GlobalUser]` directory and `[VMFile]` should be any path starting from `/home/[PrivateUser].`

Before starting, assure that the desired virtual machine is running. The virtual machine state is shown by the VirtualBox graphical user interface on the cluster (Figure 5). If the virtual machine is stopped or paused, please run it by double clicking on the corresponding icon.

Step 1:

First, you have to create a copy of your file /directory on the physical machine where virtual machines are hosted. Select the procedure based on the operative system installed on your local machine:

From Linux/ Mac OSX

From any terminal, perform the copy of your file/directory on the CNR-IMATI cluster using the following instructions:

1. Copy file
   `scp [UserFile] [GlobalUser]@150.145.8.226:/home/[GlobalUser]/[ClusterFile]`

   OR

   Copy directory
   `scp -r [UserFile] [GlobalUser]@150.145.8.226:/home/[GlobalUser]/[ClusterFile]`
2. Password `[GlobalPw]`

From Windows

To copy a file from your Windows local machine, **Bitvise SSH Client (Tunnelier)** software must be installed on your local machine. The software is available at http://www.bitvise.com/download-area.

After Tunnelier installation, please follow the instruction below:

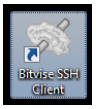

1. Open Tunnelier

2. From the Tunnelier graphical interface (Figure 6), set the following parameters and press the "Login" button:

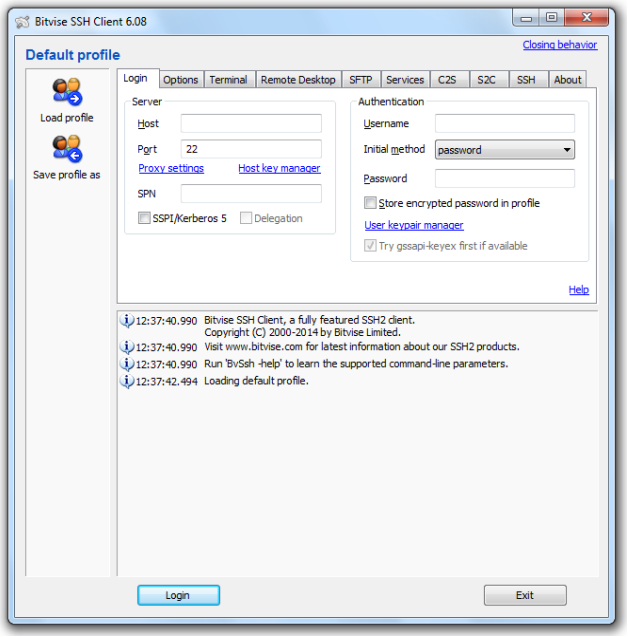

Figure 6: Tunnelier Settings

- Host: 150.145.8.226
- Port: 22
- Username: [GlobalUser]
- Password: [GlobalPw]

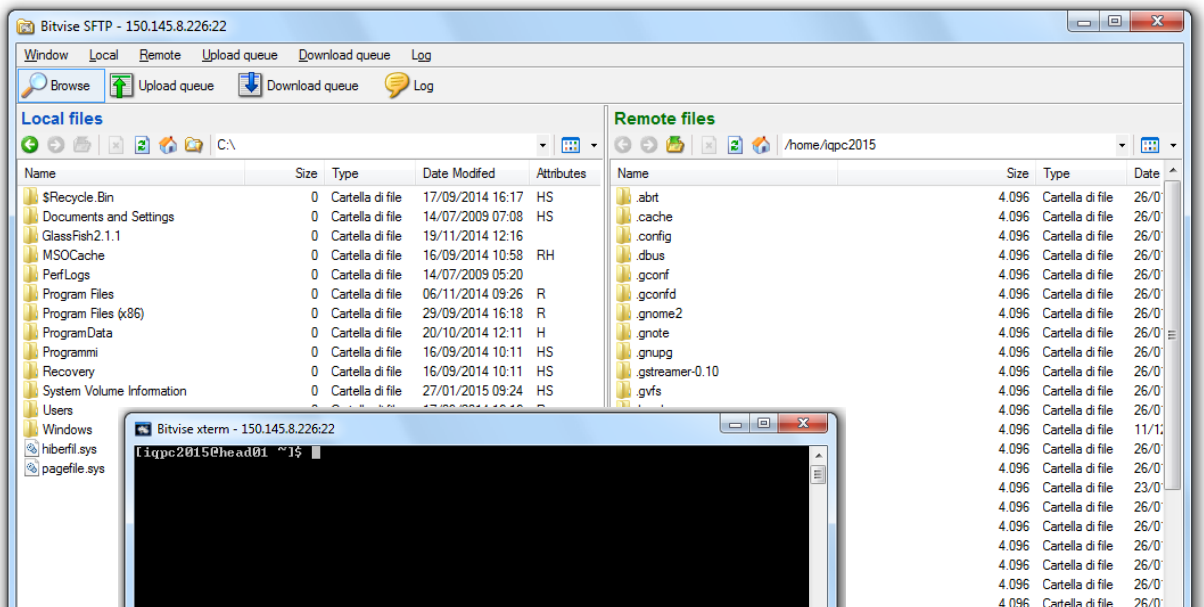

3. If required, accept the new connection. A new graphical interface is displayed (Figure 7). On the left side, the file system related to your local machine is shown. On the right side, the cluster file system is displayed. The Tunnelier command prompt is also displayed.
4. Select the file/directory `[UserFile]` you want to copy from the left side and drag and drop it into the desired directory `/home/[GlobalUser]/[ClusterFile]` on the right side.

Step 2:

The second step aims to copy the file/directory `/home/[GlobalUser]/[ClusterFile]` from the physical machine to the desired virtual machine.

In the following instructions, `[VMIP]` must be replaced with the IP address of the desired virtual machine. IP addresses are listed in section 1 (table), at the beginning of this document.

Select the procedure based on the operative system installed on the selected virtual machine:

Ubuntu virtual machine

1. From the command shell used in step 1 on your local machine:
    a. On **Linux/Mac OSX**, perform the following operations before continue
        - SSH Access `ssh -C -X [GlobalUser]@150.145.8.226`
        - Password `[GlobalPw]`
    b. On **Windows**, use the Tunnelier command shell (Figure 7)
2. Copy file `scp [ClusterFile] [PrivateUser]@[VMIP]:/home/[PrivateUser]/[VMFile]`

    OR

    Copy directory `scp -r [ClusterFile] [PrivateUser]@[VMIP]:/home/[PrivateUser]/[VMFile]`
3. Password `[PrivatePw]`

Windows virtual machine

To copy a file to a Windows virtual machine, you need to graphically access it following the procedure described in section 2 and 3. From the graphical user interface of the Windows virtual machine:

1. Open Tunnelier 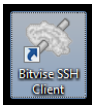

2. From the Tunnelier graphical interface (Figure 6), set the following parameters and press the "Login" button:

   - Host: 150.145.8.226
   - Port: 22
   - Username: [GlobalUser]
   - Password: [GlobalPw]

3. If required, accept the new connection.
4. A new graphical interface is displayed (Figure 7). On the left side, the file system related to the virtual machine is shown. On the right side, the cluster file system is displayed. Select the file/directory /home/[GlobalUser]/[ClusterFile] from the right side and drag and drop it into the desired directory /home/[PrivateUser]/[VMFile] on the left side.

Step 3:

The temporary copy of your file/directory on the physical machine should be removed.

From the command shell used in step 1 on your Linux/ Mac OS local machine or the Tunnelier command shell on Windows local machines (Figure 7):

1. In case the command shell is not running anymore:
   a. On **Linux/Mac OSX**, run a new terminal and perform the following operations
      - SSH Access `ssh -C -X [GlobalUser]@150.145.8.226`
      - Password `[GlobalPw]`

   b. On **Windows**, run Tunnelier and login. Use the same credentials used before (Figure 6).

2. Remove the temporary copy of your file/directory created in Step 1:
      - Remove file `rm /home/[GlobalUser]/[ClusterFile]`
      - Remove directory `rm -rf /home/[GlobalUser]/[ClusterFile]`

7.2 REPORT ON TRACK #1: EVALUATION OF AUTOMATICALLY GENERATED 2D FOOTPRINTS FROM URBAN LIDAR DATA

IQPC 2015 Track: EVALUATION OF AUTOMATICALLY GENERATED 2D FOOTPRINTS FROM URBAN LIDAR DATA

L. Truong-Hong [a, *], D. Laefer [a]

[a] Urban Modelling Group, School of Civil, Structural and Environmental Engineering and Earth Institute, University College Dublin, Belfield, Dublin, IE – (linh.truonghong, debra.laefer)@ucd.ie

Commission III, WG III/5

KEY WORDS: LiDAR data, Aerial Laser Scanning, Building Detection, Road Detection, Evaluation Strategy

ABSTRACT:

Over the last decade, several automatic approaches have been proposed to extract and reconstruct 2D building footprints and 2D road profiles from ALS data, satellite images, and/or aerial imagery. Since these methods have to date been applied to various data sets and assessed through a variety of different quality indicators and ground truths, comparing the relative effectiveness of the techniques and identifying their strengths and short-comings has not been possible in a systematic way. This open contest was designed to overcome this shortcoming. Specifically, participants were asked to submit 2D footprints (building outlines and road profiles) derived from ALS data from a highly dense dataset (approximately 225 points/m^2) across a 1km^2 of central Dublin, Ireland. The proposed evaluation strategies were designed to measure not only the capacity of each method to detect and reconstruct 2D buildings and roads but also the quality of the reconstructed building and road models in terms of shape similarity and positional accuracy. The evaluated methods will represent those submitted as part of IQPC15.

1. INTRODUCTION

The availability of three-dimensional (3D) point clouds offers a potential resource for wide ranges of applications (e.g. environmental planning and monitoring, computational simulation, disaster management, security, telecommunications, location-based services). Urban, two-dimensional (2D) footprints, which primarily include 2D footprints of buildings and the road network, play important roles in these applications and can be a major resource for generating final 3D models. For example, Laycock and Day (Laycock and Day, 2003) generated 3D building models by extruding 2D building footprints with the building height derived from aerial laser scanning (ALS) data. Similarly, a digital road map can be generated based on a 2D road profile. A number of researchers have addressed the problem of extraction and reconstruction of 2D building footprints and 2D road profiles from ALS data, satellite images, and/or aerial imagery (Boyko and Funkhouser, 2011; Clode et al., 2005; Kwak and Habib, 2014; Lafarge and Mallet, 2011; Zhang et al., 2006). Proposed methods have been tested on different data sets, and the authors have also used various evaluation criteria and ground truth resources. For example, Boyko and Funkhouser (Boyko and Funkhouser, 2011) manually generated ground truth of a road network and proposed five comparative quantities (completeness, correctness, quality, average spill size, and prevailing spill direction) to evaluate extracted roads. This lack of consensus causes difficulty in generating a consistent comparative assessment of the methods. Thus, this contest is called for participants to submit resulted 2D footprints (building outliers and road profiles) from a provided ALS datase. The contest also poses the challenge in detecting and reconstructing road profiles strictly from ALS data [several current methods required multiple data set (e.g. ALS and imagery)]. The success of this contest can provide useful information for establishing strategies for automatic urban 2D footprints from ALS data.

The contest uses a highly dense point cloud (225 million points covering approximately 1km^2 area) of Dublin, Ireland's city centre. The data have Cartesian system coordinates and intensity values and were merged from 44 flight strips. The flight plan for this dataset was design to maximize data acquisition on the building facades (Hinks et al., 2009)

The participants are asked to submit the results of automatically generated 2D building footprints (Task A) and/or 2D road profiles (Task B) from three pre-designated sub-areas of the study area. The contest organizers will evaluate submitted results based on the ground truth provided the Ordinate Survey Ireland (OSI) and OpenStreetMap (OSM). The task description, ground truth, and evaluation for each task are presented in Sections 3-5. Finally, a winner and two runners up for each task will be selected based on the overall evaluation scores.

2. RELATED WORK

Evaluating object detection has been well-studied in the remote sensing community. For a fundamental evaluation framework relating to LiDAR data, the reader can refer to one of several sources (Chuiqing et al., 2013; Heipke et al., 1997; Pfeifer et al., 2007; Rutzinger et al., 2009; Shufelt, 1999; Wiedemann et al., 1998). However, benchmarking strategies must be considered with respect to the type of object to be evaluated: buildings and road networks. As an example, as part of the EuroSDR (European Spatial Data Research – www.eurosdr.net) building extraction project, the quality, accuracy, feasibility, and economic aspects were proposed as means to evaluate the performance of semi-automatic and automatic building extraction techniques based on either ALS data or a combination of ALS data and aerial images, where corners of

* Corresponding author

walls, roofs chimneys and construction structures were measured by a Trimble 5602 DR200+ tacheometer to be used as reference points (Kaartinen et al., 2005). The project consisted of three test sites, each with typical ALS density of less than 20 points/m^2. In term of accuracy of the building outlines, the building outline errors based on LiDAR data were in a range from 20 to 150 cm, and the lengths varied from 13 to 292 cm. In addition, height differences between the extracted buildings and reference points ranged from 4 to 153 cm, while the RMSE of roof inclination was from 0.3 to 9 degrees. Furthermore, in an ISPRS benchmark project running urban object detection and 3D building reconstruction tasks, data (aerial images and ALS point clouds) were used with ALS density around 4-7 points/m^2 for Vaihingen, Germany and 6 points/m^2 for Toronto, Canada (Rottensteiner et al., 2014). Completeness, correctness and quality are crucial criteria to measure accuracy of submitted results. However, these criteria were shown in various levels to indicate the quality of the results, where the object-based system in the form of area of the object and the number of objects was used in task 1, for example. The results showed participant methods satisfactorily detected buildings larger than 50m^2. Recently, in a framework of benchmarking tests under the umbrella of IQmulus project (www.iqmulus.eu), Truong-Hong and Laefer (Truong-Hong and Laefer, 2015) proposed a shape similarity and a positional accuracy along to completeness, correctness and quality metrics, whereas the object-based system is used to indicate correctly extracted buildings. The resulted evaluation demonstrated that the error budgets involved the error of LiDAR data (acquisition and registration) and that of the submitted algorithms.

Heipke et al. (Heipke et al., 1997) proposed evaluation process to measure complete and correct road network extraction. The former aspect involving completeness, correctness and quality were based on True Positive (*TP*), False Positive (*FP*) and False Negative (*FN*) between the reference road centrelines and extracted ones. The latter aspect involved redundancy that is over-length of the extracted road, RMS difference that is based on the shortest distances between line segments of the extracted road and those of the reference ones, and gap statistics measuring the number of and length of gaps between extracted roads. However, in that work, the reference road centrelines with buffer width was used to detect matching extracted road, the direction and the shape of the extracted road were not included. The evaluation framework was then used to compare different approaches for automatic extraction of road central lines from aerial and satellite images organized by EuroSDR (Mayer et al., 2006). Completeness, correctness and RMS difference were used to evaluate performance of 6 submitted results, where the completeness and correctness were respectively around 0.7 and 0.85, while RMS difference was no more 3.74 pixels. The criteria for evaluating complete extracted road were also widely to test individually automatic road detection (Cheng et al.; Kumar et al., 2013; Miraliakbari A. et al., 2015; Narwade and Musande, 2014; Yang et al., 2013). One of which, Kumar et al. (Kumar et al., 2013), evaluated the extracted roads by using a point cloud of road edges, while Miraliakbari et al. (Miraliakbari A. et al., 2015) evaluated their work by using detected road areas. Furthermore, Boyko and Funkhouser (Boyko and Funkhouser, 2011) introduced two additional criteria called average spill size and previaling spill direction to measure discrepancies between detected and reference roads in terms of road size and direction, respectively. The pixel-based method was used to determine *TP*, *FP* and *FN* indicators.

In summary, many works have proposed benchmarks to evaluate automatically detecting building and road from LiDAR data. However, in those evaluations, criteria for evaluating complete detection of the building and roads, most involved completeness, correctness and quality metrics, while little work has been done on establishing the accuracy of the extracted objects. The motivation behind this study is to propose a robust evaluation framework indicating the level of locational deviation, the level of shape similarity, and the positional accuracy of extracted building and road networks.

3. DATA DESCRIPTION

The test area is approximately 1km^2 and consists of 205 blocks, each of which may contain in excess of a dozen buildings per block, as shown in Figure 1. The typical building is 11–15m in height, less than 5m in width, and 6–10m in length (Clarke and Laefer, 2012). The buildings are mostly closely spaced or abutting each other, with some sharing an adjoining wall, commonly referred to as a "party wall".

The dataset was acquired by ALS using the FLI-MAP 2 system, which generated 1000 pulses for each scan line. The system operated at a scan angle of 60 degrees. The quoted accuracy of the FLI-MAP 2 system is 8 cm in the horizontal plane and 5cm in the vertical direction, including both laser range and navigational errors (Hinks, 2011). Acquired points were provided in a global coordinate system with reference to the National Irish Grid (Irish Grid), relating to the use of a Global Navigation Satellite System (GNSS) to determine the aircraft position during scanning. The FLI-MAP 2 system is capable of recording up to four echoes for each emitted pulse and spectral data with intensity values.

The dominant directions of the flight tracks were chosen as north-east, north-west, south-east and south-west. The flight attitude varied between ~380-480 m (as low as possible with respect to approval by the Irish Aviation Authority), with an average elevation of ~400m. A total of 2,823 flight path points were collected during data acquisition. As a result, a point cloud was merged from 370,154 scan lines resulting in a typical density of 225 points/m^2. The echo distribution is shown in Table 1. The vast majority of points were first echoes. Secondary echoes constituted only a small portion of the points, as the overwhelming majority of surfaces in the study area were formed of solid objects (i.e. streets and buildings). For further information about this ALS data, participants are referred to Hinks (Hinks, 2011). The data set was organized into 9 tiles, each covering 500m x 500m (Figure 1), which is 5.8 Gb in size and stored with a LAS format. The data set is now publicly available.

Echo	Count	Percentage (%)
1st	217,497,975	96.33
2nd	7,902,595	3.50
3rd	383,840	0.16
4th	4,028	0.001784
Total	225,788,438	100

Table 1. Echo distribution of acquired ALS points

Three subsets of the data are used for this competition (Figure 2). Area 1 contains sparse buildings, a large green area, and trees. Area 2 has both building blocks and buildings sharing walls, as well as some trees. Area 3 contains mostly low brick buildings and no trees.

The data of each area (Area 1, 2 and 3) were extracted from the original data set and is 1.1 Gb in size in an ASCII file (Zip file), where each row represents x-, y-, z-coordinates and intensity of each data point, or in a LAS format (3.8 Gb). Either the data sets of the study area or these of the the contest are can be downloaded through the webpage of IQmulus project.

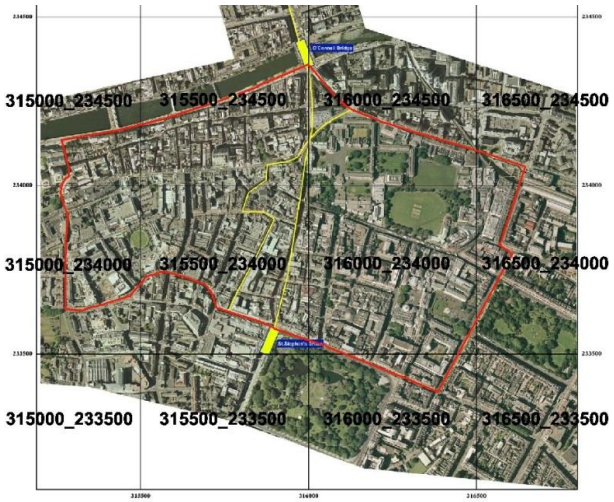

Figure 1. Acquired ALS area in Dublin central and ALS tiles (contest area outlined in red)

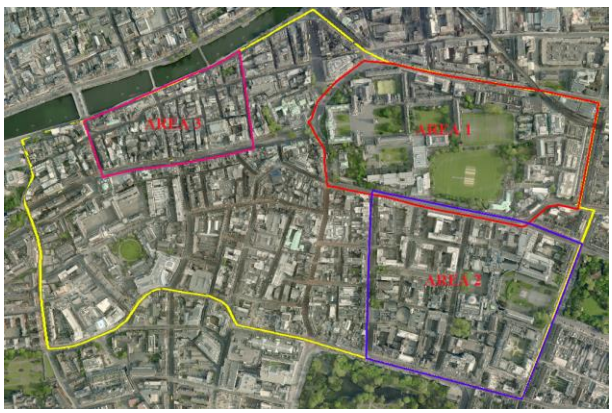

Figure 2. Designation of the three contest areas

4. TASK AND SUBMISSION

Task A is to extract a point cloud affiliated with buildings and to reconstruct 2D building footprint from these points. In urban areas, buildings are often abutting or sharing an adjoined wall. These buildings also have similar morphology (i.e. height, width or similar roof configuration), which poses a major challenge for automatic algorithms in building detection and building boundary reconstruction. Participants were asked to submit the results from their algorithms in two sets of file results: (1) ASCII files containing ALS data sets of each building, where each row represents the x-, y-, and z-coordinates of the data points and (2) ASCII files containing the building footprint describing as a polygon, where each row contains both the x- and y- coordinates of the polygon vertices. The file naming convention should be "Building_X1_Y1_X2_Y2", where the pairs X1and Y1 and X2 and Y2 are two opposite corners of the bounding box of the dataset on a horizontal plane.

Task B is to extract a point cloud of the roads and to reconstruct the 2D road profiles including the pavement edges. Similar to Task A, the participants were asked to submit two ASCII files containing: (1) ALS data points of the road network; and (2) the polygons describing pavement edges of the road network. Furthermore, the submitted files were to be named akin to Task A using the coordinates of two opposite corners of the bounding box of the road segment.

In the case that only ASCII files containing data points of either buildings or road network were submitted, the building footprints and the pavement edges of the road were to be generated by the organizer's algorithm for further evaluation.

5. GROUND TRUTH

The "ground truth" consisted of 2D footprints provided by the OSI. The 2D footprints primarily contain 2D building boundaries and road profiles (centre and edges). However, buildings and road network can be changed over time, which may not be updated in OSI 2D footprints. The building boundaries and road centres derived from the OSM were to be a supplementary resource. The 2D footprints from OSI and OSM are shown in Figure 3. Notably, the majority of footpaths in Area 1 were not available in the OSI 2D footprint. They can, however, be derived from OSM data.

Figure 3. Ground truth from OSI and OSM

6. EVALUATION STRATEGY

6.1 Task A

The evaluation process identifies the level of locational deviation, the level of shape similarity, and the positional accuracy of the extracted building footprint (*ExB*), with respect to the ground truth building (*GtB*). For the location deviation, quality indicators involving *TP*, *FP* and *FN* measure the overall extraction and reconstruction of the building footprints. These indicators can be determined after mapping extracted results

onto the *GtB*. If the object from the *ExB* matches one from the *GtB*, it is *TP*. If the object from *ExB* does not match to one from the *GtB*, it is *FP*; otherwise, if the object from *GtB* does not match one from the *ExB*, it is *FN*. These quality indicators are illustrated in Figure 4. Completeness, correctness, and quality will be the measured indicators of the submitted results, which are expressed in Eq. 1, 2 and 3.

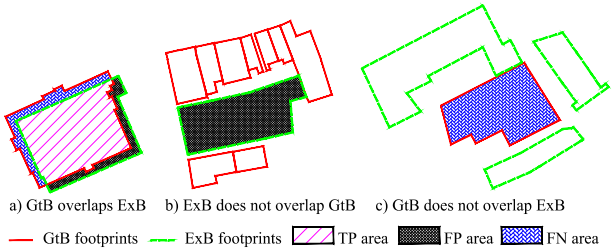

Figure 4. Illustration of determining TP, FP, and FN

$$Comp = \frac{\|TP\|}{\|TP\| + \|FN\|} \quad (1)$$

$$Corr = \frac{\|TP\|}{\|TP\| + \|FP\|} \quad (2)$$

$$Quality = \frac{\|TP\|}{\|TP\| + \|FP\| + \|FN\|} \quad (3)$$

For the level of shape similarity and positional accuracy, the building footprint from *ExB* will be considered, if this building overlaps any building from the *GtB* by a minimum of 50% in area. To measure a shape similarity, the differences in area and perimeter of each building are computed, which are given in Eq. 4 and 5.

$$\sum \delta A = \sum_{i=1}^{n} \left(A_{GtBi} - A_{ExBi} \right) \quad (4)$$

$$\sum \delta L = \sum_{i=1}^{n} \left(L_{GtBi} - L_{ExBi} \right) \quad (5)$$

where A_{GtBi} = the areas of the building footprint from *GtB*
A_{ExBi} = the areas of the building footprint from *ExB*
L_{GtBi} = the perimeter of the building footprint from *GtB*
L_{ExBi} = the perimeter of the building footprint from *ExB*
n = the number of the buildings

Subsequently, summing the absolute, mean, and standard deviation of these differences (area and perimeter) are used to express the shape similarity.

Furthermore, a positional accuracy can be described in terms of the accuracy and conciseness of the building footprint, which is performed by establishing orientation and corner errors. The orientation error (α) is the angle between L_{ExBj} (a side of the extracted building footprint i, *ExBi*) and L_{GtBi} (a side of the ground truth building footprint i, *GtBi*), where L_{GtBi} is the closest side to the L_{ExBj} (Figure 5). For details of determining a pair of L_{GtBi} and L_{ExBj}, readers can refer to Truong-Hong and Laefer (Truong-Hong and Laefer, 2015). In addition, the vertices'/corners' error (d) is defined as the Euclidean distance between the corners of the *ExBi* to its nearest corner derived from the *GtBi*. The evaluated indicators are expressed as Eq.s 6 and 7:

$$E_{orient} = \frac{\sum_{j=1}^{m} L_{ExBj} \alpha_j}{\sum_{j=1}^{m} L_{ExBj}} \quad (6)$$

$$E_{corner} = \sum_{k=1}^{n} d(p_{ExBk}, p_{GtBk}) \quad (7)$$

where L_{ExBj} = the side length of *ExBi*
α_j = the angle between the L_{PREDi} and the L_{GTi}
L_{GTi} = the side length of *GtBi*
m = the number of boundary lines in the building footprint of interest
n = the number of the corners in *ExBi*

In these error measurements, L_{ExBj} was introduced to avoid a heavy penalization for short, extracted, boundary lines (Okorn et al., 2010). Subsequently, average and standard deviations are used to measure distributions of these quantities.

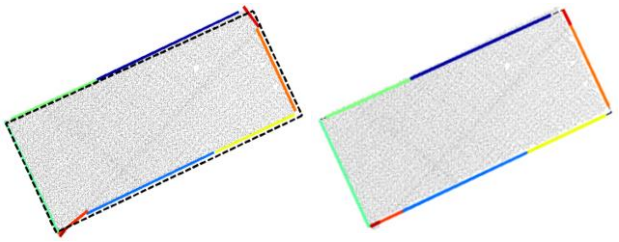

a) Overlaid boundary lines from *ExB* and *GtB* (*)
b) Illustration of a part of L_{GtBi} the closest side to the L_{ExBj} (**)

* Dashed lines are boundary lines (L_{GtB}) of *GtB* and solid color lines are the boundary lines (L_{ExB}) of *ExB*.
** Colour solid lines illustrate a part of L_{GtBi} the closest side to the L_{ExBj} in Figure 5a.

Figure 5. Illustration of determining a pair of L_{GtBi} and L_{ExBj}

6.2 Task B

Similar to Task A, the evaluation process of Task B identifies the level of locational deviation and the positional accuracy of the extracted road profile (*ExR*), with respect to the ground truth road (*GtR*). Based on the minimum bounding box of *GtR*, a 2D grid with the cell size of 1m x 1m is generated. When the *GtR* is mapped onto the 2D grid, the cell, $C_{GtRi}(x,y)$, has a value of 1, if any pavement edge or road surface of the GtR overlaps the cell (green cells in Figure 6); otherwise the value of $C_{GtRi}(x,y)$ is 0 (white cells in Figure 6).

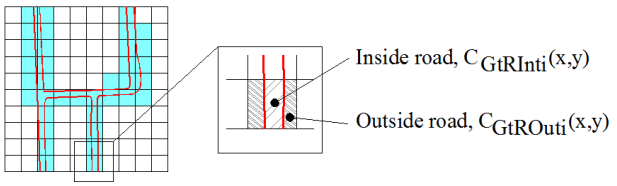

Figure 6. Classification of cells

Furthermore, if the pavement edge overlaps to $C_{GtRi}(x,y) = 1$, the cell is divided into two parts called inside road ($C_{GtRInti}(x,y)$) and outside road ($C_{GtROuti}(x,y)$, where $C_{GtRInti}(x,y)$ is a part of the cell having the centre drops between two pavement edges of the road; otherwise it is $C_{GtROuti}(x,y)$. Notably, a total area of $C_{GtRInti}(x,y)$ and $C_{GtROuti}(x,y)$ equals the cell area = $1m^2$. This rule is also applied for *ExR* when projecting *ExR* onto the 2D grid.

The locational deviation, completeness, correctness, and quality indicators mentioned in Task A are measured, where these parameters can be determined from Eq.1-3. True Positive (TP), False Positive (FP), and False Negative (FN) values are computed by comparing cell values from a pair of 2D grids represented by *GtR* and *ExR*, as expressed in Eq.s 8-10 and Figure 7.

$$\left.\begin{aligned} TP &= C_{GtRInti}(x,y) \cap C_{ExRInti}(x,y) \\ FP &= C_{ExRInti}(x,y) \setminus C_{GtRInti}(x,y) \\ FN &= C_{GtRInti}(x,y) \setminus C_{ExRInti}(x,y) \end{aligned}\right\} \text{If} \begin{cases} C_{GtRi}(x,y)=1 \\ C_{ExRi}(x,y)=1 \end{cases} \quad (8)$$

$$\left.\begin{aligned} TP &= 0 \\ FP &= 0 \\ FN &= C_{GtRInti}(x,y) \end{aligned}\right\} \text{If} \begin{cases} C_{GtRi}(x,y)=1 \\ C_{ExRi}(x,y)=0 \end{cases} \quad (9)$$

$$\left.\begin{aligned} TP &= 0 \\ FP &= C_{ExRInti}(x,y) \\ FN &= 0 \end{aligned}\right\} \text{If} \begin{cases} C_{GtRi}(x,y)=0 \\ C_{ExRi}(x,y)=1 \end{cases} \quad (10)$$

where C_{GtRi} = the cell value from GtR
C_{ExRi} = the cell value from ExR
$C_{GtRInti}$ = the areas of a part of C_{GtRi} inside GtR
$C_{ExRInti}$ = the areas of a part of C_{ExRi} inside ExR

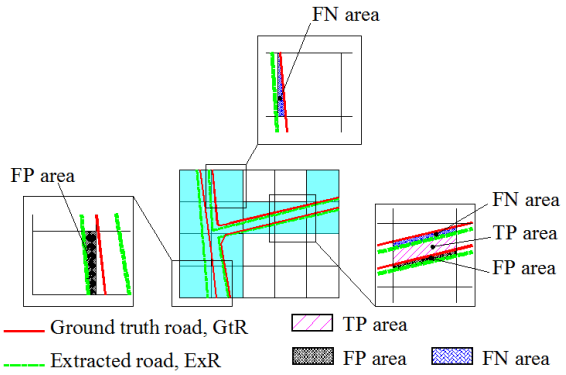

Figure 7. Illustration of computing TP, FP and FN areas

The positional accuracy can be determined through differences in location and orientation of the road edges between the ground truth and extracted roads. A distance and angle between the road edges from the ground truth and the extracted results are proposed to measure those differences. A pair of road edges (L_{GtRi} from *GtR* and L_{ExRi} from *ExR*) is initially extracted. For that, if $C_{GtRi}(x,y) = 1$, a pavement edge segment from *GtR* overlapping $C_{GtRi}(x,y)$ is computed, which is called L_{GtRi}. Then, if the angle between the L_{GtRi} and a horizontal direction (n_x = [1,0]) is less than or equal to 45 degrees, a pavement edge segment of the *ExR* on the same vertical grid to the $C_{GtRi}(x,y)$ closest to the L_{GtRi} is the L_{ExRi}. Otherwise, the pavement edge segment of the *ExR* on the horizontal grid to the $C_{GtRi}(x,y)$ closest to the L_{GtRi} is the L_{ExRi} (Figure 8). From the pair of the road edge segments, the distance and orientation errors (L_{GtRi} and L_{ExRi}, respectively) can be computed according to Eq.s 11 and 12, where the distance between L_{GtRi} and L_{ExRi} is the distance between the middle of the L_{ExRi} and the L_{GtRi}.

$$E_{distR} = \frac{\sum_{i=1}^{n} L_{ExRi}\, d(L_{GtRi}, L_{ExRi})}{\sum_{i=1}^{n} L_{ExRi}} \quad (11)$$

$$E_{orientR} = \frac{\sum_{i=1}^{n} L_{ExRi}\, \alpha_i}{\sum_{i=1}^{n} L_{ExRi}} \quad (12)$$

where n = the number of pairs of the road edge segments
α_j = the angle between the L_{GtRi} and the L_{ExRi}

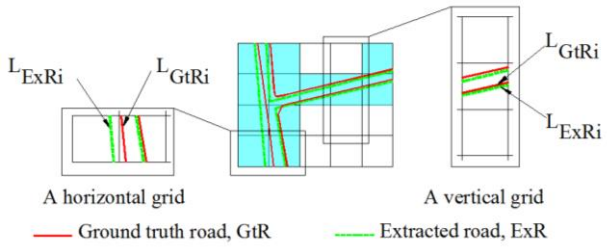

Figure 8. Illustration of determining a pair of road edge segments (L_{GtRi} and L_{ExRi})

Finally, the winners of each task are to be selected based on the overall evaluation of the output quality, where all evaluated quantities are weighted equally.

7. CONCLUSION

Many automatic approaches have been proposed to detect and reconstruct building and road profiles from ALS data. Previously, these methods were evaluated by using different data sets associated with various different criteria and ground truths. That precludes a rigorous comparison of the advantages and disadvantages of each method. This paper presents the objectives of the track in the IQPC 2015 contest related to automatic detection and reconstruction of buildings and road networks. The contest was run on dataset consisting of ALS data captured over 1km^2 of the Dublin's city centre with a typical data density of 225 points/m^2. The success of this contest can provide into establishing strategies for automatic urban 2D footprints from ALS data.

An evaluation strategy was proposed to benchmark the results in terms of the capacity of the submitted results in detecting and reconstructing building and road outlines. Unlike existing evaluation frameworks, where a level of a complete detection and reconstruction of approaches is considered through completeness, correctness and quality metrics, this study proposes a robust evaluation process indicating the level of locational deviation, the level of shape similarity, and the positional accuracy of the extracted building footprints and road profiles, with respect to the ground truth building and road. This work can provide performance measures to evaluate participant methods in term of an accuracy of object detection and reconstruction. The contest was launched in March 2015. The test datasets remain available on the webpage of the track. Participants are welcome to submit for future evaluation.

ACKNOWLEDGEMENTS

Data acquisition was generously supported by Science Foundation Ireland through PICA program. This work was funded by the European Union through ERC program. The authors gratefully acknowledge this support.

REFERENCES

Boyko, A., Funkhouser, T., 2011. Extracting roads from dense point clouds in large scale urban environment. ISPRS Journal of Photogrammetry and Remote Sensing 66, S2-S12.

Cheng, L., Wu, Y., Wang, Y., Zhong, L., Chen, Y., Li, M., Three-dimensional reconstruction of large multilayer interchange bridge using airborne Lidar data. IEEE Journal of Selected Topics in Applied Earth Observations and Remote Sensing 8, 691-708.

Chuiqing, Z., Jinfei, W., Lehrbass, B., 2013. An Evaluation System for Building Footprint Extraction From Remotely Sensed Data. Selected Topics in Applied Earth Observations and Remote Sensing, IEEE Journal of 6, 1640-1652.

Clarke, J., Laefer, D.F., 2012. Generation of a Building Typology for Urban Tunnelling Risk Assessment, Bridge and Concrete Research in Ireland, Dublin, Ireland.

Clode, S., Rottensteiner, F., Kootsookos, P.J., 2005. Improving city model determination by using road detection from lidar data, Joint Workshop of ISPRS and the German Association for Pattern Recognition (DAGM),'Object Extraction for 3D City Models, Road Databases and Traffic Monitoring-Concepts, Algorithms, and Evaluation'(CMRT05).

Heipke, C., Mayer, H., Wiedemann, C., Jamet, O., 1997. Evaluation of automatic road extraction. International Archives of Photogrammetry and Remote Sensing 32, 151-160.

Hinks, T., 2011. Geometric Processing Techniques for Urban Aerial Laser Scan Data. University College Dublin.

Hinks, T., Carr, H., Laefer, D.F., 2009. Flight optimization algorithms for aerial LiDAR capture for urban infrastructure model generation. Journal of Computing in Civil Engineering 23, 330-339.

Kaartinen, H., Hyyppä, J., Gülch, E., Vosselman, G., Hyyppä, H., Matikainen, L., Hofmann, A.D., Mäder, U., Persson, Å., Söderman, U., Elmqvist, M., Ruiz, A., Dragoja, M., Flamanc, D., Maillet, G., Kersten, T., Carl, J., Hau, R., Wild, E., Frederiksen, L., Holmgaard, J., 2005. Accuracy of 3D city models: EuroSDR comparison, the ISPRS Workshop Laser scanning. ISPRS, pp. 227-232.

Kumar, P., McElhinney, C.P., Lewis, P., McCarthy, T., 2013. An automated algorithm for extracting road edges from terrestrial mobile LiDAR data. ISPRS Journal of Photogrammetry and Remote Sensing 85, 44-55.

Kwak, E., Habib, A., 2014. Automatic representation and reconstruction of DBM from LiDAR data using Recursive Minimum Bounding Rectangle. ISPRS Journal of Photogrammetry and Remote Sensing 93, 171-191.

Lafarge, F., Mallet, C., 2011. Building large urban environments from unstructured point data, Computer Vision (ICCV), 2011 IEEE International Conference on, pp. 1068-1075.

Laycock, R.G., Day, A.M., 2003. Automatically generating large urban environments based on the footprint data of buildings, Proceedings of the eighth ACM symposium on Solid modeling and applications. ACM, Seattle, Washington, USA, pp. 346-351.

Mayer, H., Hinz, S., Bacher, U., Baltsavias, E., 2006. A test of automatic road extraction approaches. International Archives of Photogrammetry, Remote Sensing, and Spatial Information Sciences 36, 209-214.

Miraliakbari A., Hahn, M., Sok, S., 2015. Automatic Extraction of Road Surface and Curbstone Edges from Mobile Laser Scanning Data. ISPRS - International Archives of the Photogrammetry, Remote Sensing and Spatial Information Sciences XL-4/W5, 119-124.

Narwade, R.D., Musande, V., 2014. Road extraction from airborne LiDAR data using SBF and CD-TIN, Advances in Computing, Communications and Informatics (ICACCI, 2014 International Conference on. IEEE, pp. 1009-1014.

Okorn, B., Xiong, X., Akinci, B., Huber, D., 2010. Toward automated modeling of floor plans, Symposium on 3D Data Processing, Visualization and Transmission, Paris, France p. 8.

Pfeifer, N., Rutzinger, M., Rottensteiner, F., Muecke, W., Hollaus, M., 2007. Extraction of building footprints from airborne laser scanning: Comparison and validation techniques, Urban Remote Sensing Joint Event, 2007, pp. 1-9.

Rottensteiner, F., Sohn, G., Gerke, M., Wegner, J.D., Breitkopf, U., Jung, J., 2014. Results of the ISPRS benchmark on urban object detection and 3D building reconstruction. ISPRS Journal of Photogrammetry and Remote Sensing 93, 256-271.

Rutzinger, M., Rottensteiner, F., Pfeifer, N., 2009. A Comparison of Evaluation Techniques for Building Extraction From Airborne Laser Scanning. Selected Topics in Applied Earth Observations and Remote Sensing, IEEE Journal of 2, 11-20.

Shufelt, J.A., 1999. Performance evaluation and analysis of monocular building extraction from aerial imagery. Pattern Analysis and Machine Intelligence, IEEE Transactions on 21, 311-326.

Truong-Hong, L., Laefer, D.F., 2015. Quantitative evaluation strategies for urban 3D model generation from remote sensing data. Computers & Graphics.

Wiedemann, C., Heipke, C., Mayer, H., Jamet, O., 1998. Empirical evaluation of automatically extracted road axes. Empirical Evaluation Techniques in Computer Vision, 172-187.

Yang, B., Fang, L., Li, J., 2013. Semi-automated extraction and delineation of 3D roads of street scene from mobile laser scanning point clouds. ISPRS Journal of Photogrammetry and Remote Sensing 79, 80-93.

Zhang, K., Yan, J., Chen, S.-C., 2006. Automatic construction of building footprints from airborne LIDAR data. Geoscience and Remote Sensing, IEEE Transactions on 44, 2523-2533.

7.3 REPORT ON TRACK #2: WATER DETECTION AND CLASSIFICATION ON MULTISOURCE REMOTE SENSING AND TERRAIN DATA

IQPC 2015 TRACK: WATER DETECTION AND CLASSIFICATION ON MULTI-SOURCE REMOTE SENSING AND TERRAIN DATA

A. Olasz[a], D. Kristóf[a]*, M. Belényesi[a], K. Bakos[a],
Z. Kovács[b], B. Balázs[b], Sz. Szabó[b]

[a] FÖMI, Institute of Geodesy, Cartography and Remote Sensing, 1149 Budapest, Hungary - kristof.daniel@fomi.hu
[b] Department of Physical Geography and Geoinformation Systems, University of Debrecen, Hungary - szabo.szilard@science.unideb.hu

Commission VI, WG VI/4

KEY WORDS: IQmulus Processing Contest, Remote Sensing, Water detection and classification, Multi-source remote sensing data processing, Resource optimization, R programming

ABSTRACT:

Since 2013, the EU FP7 research project "IQmulus" encourages the participation of the whole scientific community as well as specific user groups in the IQmulus Processing Contest (IQPC). This year, IQPC 2015 consists of three processing tasks (tracks), from which "Water detection and classification on multi-source remote sensing and terrain data" is introduced in the present paper. This processing track addresses a particular problem in the field of big data processing and management with the objective of simulating a realistic remote sensing application scenario. The main focus is on the detection of water surfaces (natural waters, flood, inland excess water, other water-affected categories) using remotely sensed data. Multiple independent data sources are available and different tools could be used for data processing and evaluation. The main challenge is to identify the right combination of data and methods to solve the problem in the most efficient way. Although the first deadline for submitting track solutions has passed and the track has been successfully concluded, the track organizers decided to keep the possibility of result submission open to enable collecting a variety of approaches and solutions for this interesting problem.

1. INTRODUCTION

1.1 Introduction

The IQmulus EU FP7 project (http://www.iqmulus.eu) encourages the participation of the whole scientific community as well as specific user groups and research teams in the framework of IQmulus Processing Contest (IQPC) since 2013. Software performance is evaluated through the creation of benchmarks and evaluation methodologies specific for selected processing tasks (IQmulus Tracks). Beside the selection of test datasets with a ground truth, IQPC supports the usage of a common infrastructure where the executables submitted are run and results are collected and evaluated.

In 2015, IQPC is a theme of a Special Session in the ISPRS Geospatial Week in the GeoBigData Workshop and track reports will be reviewed to be included in the conference proceedings (ISPRS Archives). At the IQPC Special Session 30 minutes presentations will be held by the track organizers to report about the proposed solutions about each submission as well.

This paper introduces the track named "Water detection and classification on multi-source remote sensing and terrain data". This track has been defined by the Institute of Geodesy, Cartography and Remote Sensing, Hungary (FÖMI), a consortium partner in the IQmulus project. The challenge is to address the problem of detecting water surfaces and different categories of water-affected soils and vegetation based on a variety of remotely sensed data of different resolutions.

1.2 Background

Detection and monitoring of various water surfaces has been a challenge for a long time in remote sensing data processing. A large number of studies are available in the relevant literature dealing with water and wetness detection and monitoring for land management and conservation (e.g. Li et al. 2013; Rokni et al. 2014). Numerous different types of RS data are useful for some kind of water detection; however the accuracy is highly dependent on the input source, the processing methodology and in particular the combination of the two.
In real-life situations, a balance is achieved by creating a processing chain consisting of different methods and input sources and spatially aware algorithms are used to combine the tools to provide a result of sufficient information content. However a very challenging task is to optimize the resources for the tasks.

1.3 Objectives

The goal of this track is to detect water-related thematic classes in a specific area in Hungary. The track leader provides a wide array of remote sensing data covering the area in concern, including:

1. High-resolution aerial hyperspectral imagery
2. High-resolution visible (RGB) orthophotos
3. Terrain model (DTM) and surface model (DSM) derived from airborne LiDAR point clouds,
4. Medium-resolution (Landsat 8) satellite imagery.

* Corresponding author

The participants have to provide thematic maps with a set of pre-defined categories. A set of calibration and validation samples will be provided to train and validate the various processing chains, and final evaluation will be carried out by the track leader (FÖMI) using independent samples. Competitive solutions have to fulfil the below criteria:

1. Create the best possible classification using the simplest set/combination of input sources
2. Try to reduce the number of input data for the processing
3. Develop algorithms that are fast to run
4. Find the best balance of complexity and accuracy (maximize efficiency) during the data processing

2. DATA DESCRIPTION

2.1 Study area description

The study area is located in the North-East part of Hungary, along the river Bodrog (Figure 1) which is a tributary to the river Tisza. The river Bodrog is crosses the Slovak–Hungarian border at the village of Felsőberecki (near Sátoraljaújhely) in Hungary, and continues its flow through the Hungarian county Borsod-Abaúj-Zemplén, until it joins the river Tisza in Tokaj city. The lowest point of the study area is on 77,19 m, while the highest point is on 258,73 m above the sea level. The study area is often affected by floods and inland excess water by the two rivers.

Figure 1. The location of the study area in Hungary

The study area is divided into three parts (Figure 2):

1. Area A: the full study area with medium-resolution Landsat 8 coverage

2. Areas B and C: two sub-areas with full high-resolution data coverage (hyperspectral and multispectral airborne data, DTM and DSM).

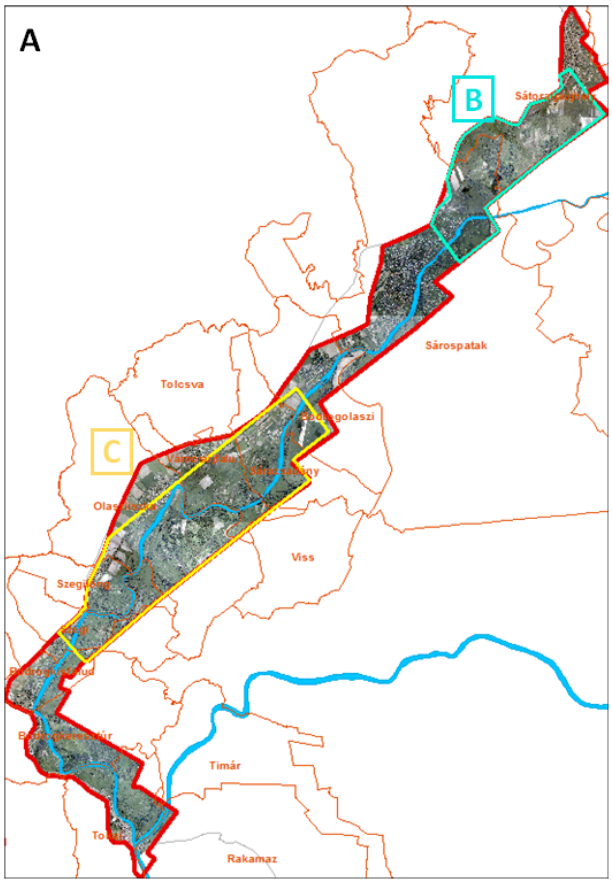

Figure 2. Study area

The participants have to provide thematic maps for each of the areas (A, B and C) with the below categories:

1. Water surfaces (code: 1)
2. Wet/waterlogged soils (code: 2)
3. Soils not directly affected by water (code: 3)
4. Vegetation standing in water (code: 4)
5. Vegetation not directly affected by water (code: 5)
6. Other (code: 0)

For each area, a set of training and verification samples being provided by the track leader in vector format, covering each of the above thematic categories. The participants can use the samples to train the classification algorithms and to verify the results. Areas with both high- and low-resolution data coverage (B and C) can be used to tune the algorithms for better performance on the larger area with only Landsat data (area A, Figure 3).

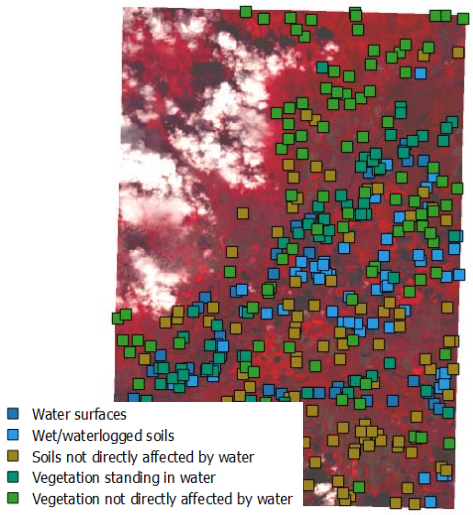

Figure 3. Distribution of categorized point dataset (reference) for the study area A.

2.2 Input data description

For area 'A' Landsat 8 data is provided, whereas hyperspectral images, LiDAR-derived Digital Surface (DSM), Terrain Model (DTM) and orthophotos (RGB) are additionally provided for areas 'B' and 'C'.

2.2.1 Hyperspectral images

Hyperspectral images are provided as georeferenced (UTM34N/WGS84) radiance data in *.dat (ENVI) format (16 bit BSQ) containing 128 bands (Figure 4). Additional technical details on spectral and spatial resolution and accuracy are the follows:

1. Instrumentation / camera: aerial hyperspectral instrument (AISA Eagle)
2. Spectral range: approx. 400-1000 nm (visible and reflected (near) infrared, VIS / VNIR)
3. Spectral resolution: 5 nm
4. Spatial resolution: 1.5 m / pixel
5. Spatial accuracy: 2.5 m (RMSE)

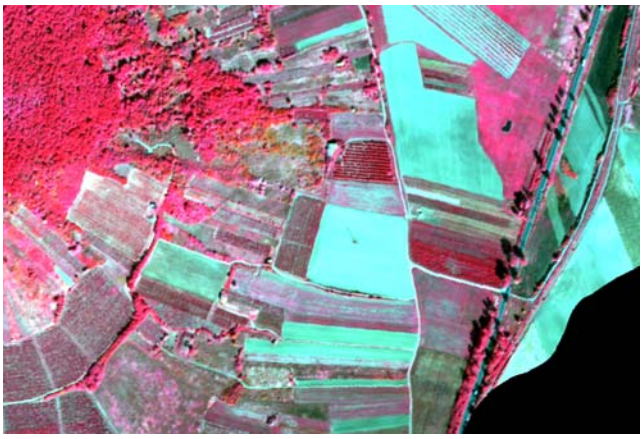

Figure 4. Hyperspectral image

2.2.2 Digital orthophotos

Multispectral (visible, RGB) orthophoto is provided as georeferenced (UTM34N/WGS84) and radiometrically corrected TIFF (Figure 5). The spatial resolution is 15 cm/pixel with spatial accuracy of 30 cm (RMSE)

Figure 5. Orthophoto

2.2.3 Digital Terrain Model (DTM)

The Digital Terrain Model is generated from aerial laser scanner (ALS) data, with gap filling by appropriate interpolation. Data is provided as georeferenced (UTM34N/WGS84), unsigned long integer TIFF. Data content is height values in cm, interpreted over Baltic Sea level. The Spatial resolution is 1 meter / pixel with spatial accuracy of 30 cm.

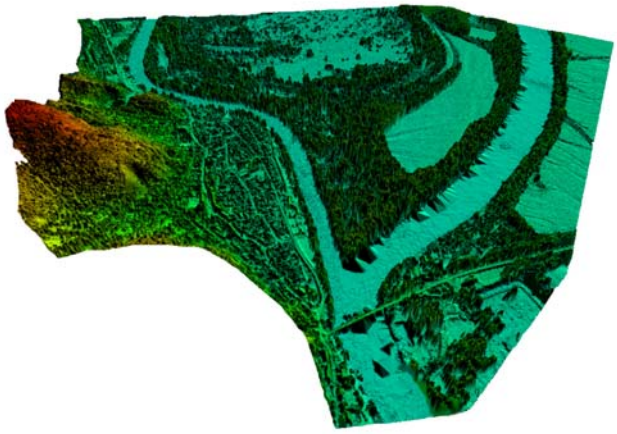

Figure 6. Digital Terrain Model for the conjunction of River Tisza and Bodrog at the city of Tokaj

2.2.4 Landsat 8 Data

For the whole area of interest we provide a subset of Landsat 8 imagery. The data is processed as standard Level-1 (orthorectified, terrain corrected), and provided as georeferenced (UTM34N/WGS84) and radiometrically corrected TIFF (unsigned integer 32 bit). Landsat 8 Operational Land Imager (OLI) images consist of nine spectral bands with a spatial resolution of 30 meters for Bands 1 to 7 and 9. New band 1 (ultra-blue) is useful for coastal and aerosol studies. New band 9 is useful for cirrus cloud detection.
The resolution for Band 8 (panchromatic) is 15 meters.
Thermal Infrared Sensor (TIRS) bands 10 and 11 are useful in providing more accurate surface temperatures and are collected at 100 meters, resampled to 30 meters.

3. EVALUATION

Participants had to submit the following material:

1. Georeferenced thematic rasters in GeoTIFF format, containing the codes of thematic categories as described above
2. Concise description of the whole methodology and processing chain (including algorithms and parameters, with references to relevant literature wherever available)

Evaluation and scoring was based upon the complexity, time- and resource efficiency of the methodology and the data requirement for processing.

4. TRACK RESULTS

Due to the deadline of the admission for the IQPC 2015 we have received one application to be presented at the GeoBigData Workshop. It was submitted by the team of the *Department of Physical Geography and Geoinformation Systems, University of Debrecen*. The team consist of three members: Zoltán Kovács, Boglárka Balázs and Szilárd Szabó. From this point on, in this paper we refer to them as "the Debrecen team".
As several possible participants have shown interest we are open to receive more solutions for the task published in Track 2 until the end of 2015 (but outside of the scope of the GeoBigData Workshop and IQPC 2015).

4.1 Solution provided by the Debrecen team

4.1.1 Introduction

The aim of this contest track was to detect water surfaces using remotely sensed data. In our research we attempted to reduce the number of input data, therefore this task was approached from multispectral data source, so the medium-resolution OLI multispectral bands of Landsat 8 satellite imagery was used exclusively. Decreasing the processing time and human interaction, most of the steps were programmed in python and R programming languages.

According to the Track 2, the following categories were distinguished:

- Water surfaces (code: 1)
- Wet/waterlogged soils (code: 2)
- Soils not directly affected by water (code: 3)
- Vegetation standing in water (code: 4)
- Vegetation not directly affected by water (code: 5)
- Other (code: 0)

4.1.2 Data processing

During data processing the training and two test datasets were available as ESRI point shape files, which were used to train the classification methods and verify the performance of the predictions. Intensity values of these pixels were extracted from the OLI multispectral bands (Band1-Band7, Band9) in ArcGIS 10.2. and saved as *.csv text files by using our python script.
The *.csv files were imported into an Excel workbook, where data was processed by HypDA (Hyperspectral Data Analyst) MS Excel add-in which was developed at Department of Physical Geography and Geoinformation Systems, University of Debrecen (Kovács & Szabó, 2013). It is being specially developed and designed for multispectral and hyperspectral data processing. HypDA is able to conduct hypothesis testing (e.g. Kruskal-Wallis test), separability testing (e.g. Jeffries-Matusita distance) and some classification procedures (e.g. minimum distance, Mahalanobis distance) for distinguishing the predefined classes by using self-generated spectral indices. HypDA workbooks contains specific worksheets, where the first two contains the intensity values and nominal or scale properties, the others the processing chain; one of them calculates matrices with all possibilities of bands to get the best available spectral indices, the other worksheets store the best values of matrices and show the detailed statistical background of the investigations of that certain models. In this case these methods were used to create spectral indices for each category for further investigations (classification in R). Our HypDA-based spectral indices were the following for the Landsat image:

- Code 1 <- (B5 - B3)/(B5 + B5)
- Code 2 <- (B9 - B1)/(B5 + B5)
- Code 3 <- (B7 - B2)/(B4 + B4)
- Code 4 <- (B7 - B1)/(B5 + B5)
- Code 5 <- (B5 - B3)/(B2 + B7)

R is free statistical software with command line interface (R Core Team, 2014). It is becoming more and more popular among scientific environments. It has many downloadable libraries providing widespread field of application. One of them, the Rattle was especially developed for data mining (Williams, 2011). Decision tree (DT, Mingers, 1989), Random forest (RF, Ho, 1995), Support Vector Machine (SVM, Nguyen and de la Torre, 2010) and Generalised Linear models (GLM, Bishop, 2006) can be used on training set to set classification rules for predicting classes for test sets and validation sets. For these models the target variable was the "gridcode" variable from shape files, the input variables were the spectral indices determined by HypDA. These indices were calculated for all test sets, training set and for the whole Landsat dataset. In order to verify the applied models, kappa indices and overall accuracy were calculated for all applied methods and all test sets (test1, test2 and test1+test2) from the confusion matrices of the models.
In order to create a classified geotiff map, the Landsat image was exported as ASCII file storing all intensity values of pixels. The lines of file represented individual pixels with the same structures as the training and test sets, therefore it was able to use as validation dataset for our investigations and Rattle was able to assign classes for each pixel. Beside the predicted classes, R can also determine the probabilities of classes for each pixel. In this way not only the classified pixels can be exported into text files, but the maximum probabilities of classes can be also saved and probability maps can be created for each method. Probabilities were cut by a predefined critical value (0.95), thus pixels with smaller probability were classified as "Others".
Classification procedure was summarized in the Fig. 7.
Besides masking the values having <95% classification probability, we masked the areas covered by clouds, too. Altogether 125 test data point fell in cloud covered areas; therefore, we provide two solutions for the accuracy assessment:

- (1) calculations including all test points (test1, test2 and test1+test2)
- (2) calculations omitting the cloud covered areas.

In our understanding, solution (2) is more reliable, as pixels covered by clouds are biased and have distorted intensity values.

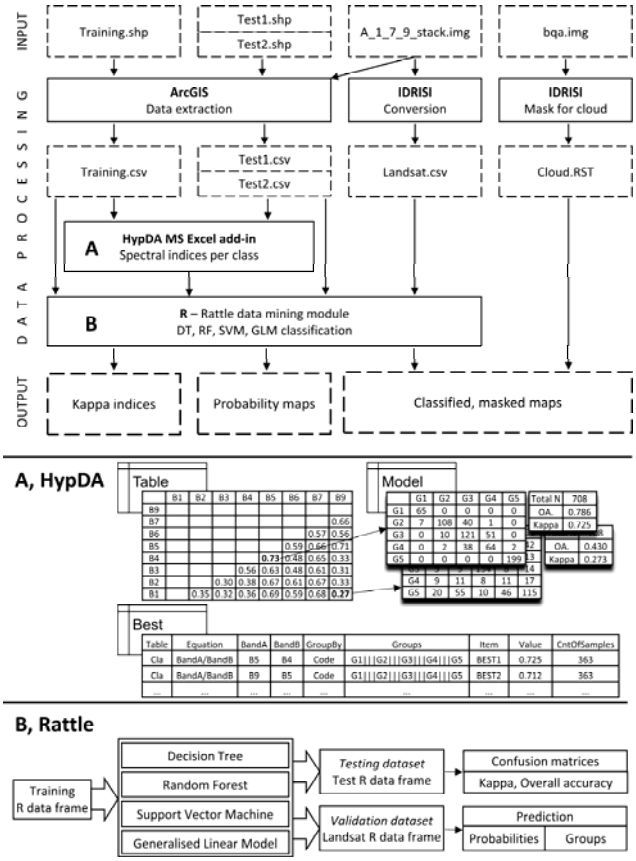

Figure 7. Classification procedure by the Debrecen team

4.1.3 Accuracy assessment

We compared the performance of the classification techniques based on Kappa values and found the GLM (General Linear Model) having the best performance. Confusion matrix and the accuracy statistics are shown on Figure 8.

Confusion matrix on the test sets without cloud mask

Test set 1 and Test set 2					
	1	2	3	4	5
1	70	2	0	0	0
2	5	107	4	4	0
3	0	6	191	2	0
4	0	4	1	111	0
5	0	0	1	0	200
Overall accuracy: 0.959					
Kappa: 0.956					

Test set 1					
	1	2	3	4	5
1	39	2	0	0	0
2	2	48	2	2	0
3	0	2	98	1	0
4	0	3	0	52	0
5	0	0	0	0	107
Overall accuracy: 0.960					
Kappa: 0.958					

Test set 2					
	1	2	3	4	5
1	31	0	0	0	0
2	3	59	2	2	0
3	0	4	93	1	0
4	0	1	1	59	0
5	0	0	1	0	93
Overall accuracy: 0.957					
Kappa: 0.955					

Confusion matrix on the test sets with cloud mask

Test set 1 and Test set 2					
	1	2	3	4	5
1	65	3	0	0	0
2	0	78	0	0	0
3	0	6	169	0	0
4	0	1	1	96	0
5	0	0	0	0	199
Overall accuracy: 0.991					
Kappa: 0.991					

Test set 1					
	1	2	3	4	5
1	37	1	0	0	0
2	0	37	0	0	0
3	0	0	86	0	0
4	0	3	0	44	0
5	0	0	0	0	106
Overall accuracy: 0.996					
Kappa: 0.996					

Test set 2					
	1	2	3	4	5
1	28	2	0	0	0
2	0	41	0	0	0
3	0	0	83	0	0
4	0	1	1	52	0
5	0	0	0	0	93
Overall accuracy: 0.986					
Kappa: 0.986					

Figure 8. Confusion matrix and accuracy statistics of the solution provided by the Debrecen team

5. CONCLUSIONS

The Debrecen team has provided an elegant solution to the challenge raised in the context of water detection and classification in the frame of IQmulus Processing Contest 2015. Their solution is based on Landsat-8 imagery and does not use any other input data, yet provides very accurate results for the desired categories.

Although the first deadline for submitting track solutions has passed and the track has been successfully concluded, the track organizers decided to keep the possibility of result submission open to enable collecting a variety of approaches and solutions for this interesting problem. Potential additional solutions would also be presented in the frame of the track summary presentation at the GeoBigData workshop and published at the project homepage.

ACKNOWLEDGEMENTS

IQmulus (full name: A High-volume Fusion and Analysis Platform for Geospatial Point Clouds, Coverages and Volumetric Data Sets) is a 4-year Integrating Project (IP) partially funded by the European Commission under the Grant Agreement FP7-ICT-2011-318787. It is positioned in the area of Intelligent Information Management within the ICT 2011.4.4 Challenge 4: Technologies for Digital Content and Languages. IQmulus started on November 1, 2012, and will finish on October 31, 2016.

REFERENCES

IQmulus Processing Contest 2015. Water detection and classification on multi-source remote sensing and terrain data Proposal [Online]. Available at http://iqmulus.eu/iqpc/iqmulus-processing-contest-2015 [June 25, 2015].

D.8.8.2 Report on IQmulus Processing Contest – year 2 [Online]. Available at http://iqmulus.eu/dynamic/document/D8.8.2_Report_on_the_IQmulus_Processing_Contest_Year_2.pdf [June 25, 2015].

Bishop, C.M., 2006. Pattern recognition and Machine Learning. Springer, Cambridge, pp. 729

Ho, T. K., 1995. Random decision forests, in Proceedings of the 3rd International Conference on Document Analysis and Recognition, Montreal, Canada, IEEE Computer Society, pp. 278-282.

Kovács, Z., Szabó, Sz., 2013. Interactive spectral evaluation in Excel environment – add-in for hyperspectral data processing. In Lóki, J. ed.: Proceedings of 4th Hungarian Conference and Exhibition of Geoinformation Science, Debrecen, Hungary, pp. 251-255. (in Hungarian)

Li, W., Du, Z., Ling, F., Zhou, D., Wang, H., Gui, Y., Sun, B., Zhang, X., 2013. A Comparison of Land Surface Water Mapping Using the Normalized Difference Water Index from TM, ETM+ and ALI. Remote Sensing 5(11) pp. 5530-5549.

Mingers, J., 1989. An empirical comparison of selection measures for decision-tree induction. Machine Learning 3(4), pp. 319-342.

Nguyen, M.H., De la Torre, F., 2010. Optimal feature selection for support vector machines, Pattern Recognit.43 (3), pp. 584-591.

R Core Team, 2014. R: A language and environment for statistical computing. R Foundation for Statistical Computing, Vienna, Austria. Available at http://www.R-project.org/

Rokni, K., Ahmad, A., Selamat, A., Hazini, S. 2014. Water Feature Extraction and Change Detection Using Multitemporal Landsat Imagery. Remote Sensing 6(5) pp. 4173-4189.

Williams, G. J., 2011. Data Mining with Rattle and R: The Art of Excavating Data for Knowledge Discovery, Use R!, Springer.

7.4 REPORT ON TRACK #3: TREE SEPARATION AND CLASSIFICATION IN MOBILE MAPPING LIDAR DATA

IQPC 2015 TRACK:
TREE SEPARATION AND CLASSIFICATION IN MOBILE MAPPING LIDAR DATA

Ben Gorte [a], Sander Oude Elberink [b], Beril Sirmacek [a], Jinhu Wang [a]
[a] Dept. of Geoscience and Remote Sensing, TU Delft, the Netherlands, {b.g.h.gorte, b.sirmacek, jinhu.wang}@tudelft.nl
[b] ITC, University of Twente, the Netherlands, s.j.oudeelberink@utwente.nl

Commission III, WG III/5

KEY WORDS: Mobile mapping systems, Lidar, Tree separation, Classification.

ABSTRACT:

The European FP7 project IQmulus yearly organizes several processing contests, where submissions are requested for novel algorithms for point cloud and other *big* geodata processing. This paper describes the set-up and execution of a contest having the purpose to evaluate state-of-the-art algorithms for Mobile Mapping System point clouds, in order to detect and identify (individual) trees. By the nature of MMS these are trees in the vicinity of the road network (rather than in forests). Therefore, part of the challenge is distinguishing between trees and other objects, such as buildings, street furniture, cars etc. Three submitted segmentation and classification algorithms are thus evaluated.

1. INTRODUCTION

Analysis of laser-generated point clouds for forest applications has already gained a good reputation[1] . For the purpose of forest inventories, for example, laser data are being analysed to estimate the number of trees in a forest, identify species, and estimate wood volumes. For large forest areas airborne laser scanning is the preferred data source, whereas for detailed studies at individual tree level also terrestrial laser scanning is being used.

Mobile mapping systems (MMS) typically integrate laser scanners, cameras and navigation sensors (GPS, IMU and odometers) [2]. They are mounted on cars or trucks and capture data while driving. Initiatives from various agencies and companies using different MMS equipment are currently being executed and will eventually capture the entire road network with the surrounding objects.

At the same time there is an interest of municipalities and other authorities to form databases ("cadasters") of the trees in the public space they manage. Many trees are located along streets and roads, and are therefore capture in MMS campaigns. In order to record information at the individual tree level, it is necessary to identify those individual trees in the data. This issue is, for example, addressed at boomregister.nl for the entire Netherlands.

2. TREE CLASSIFICATION AND SEPARATION CONTEST

IQmulus is a European FP7 project aiming at offering a high-volume fusion and analysis platform for geospatial point clouds, coverages and volumetric data sets. The project includes organizing IQmulus Processing Contests (IQPC). This year's contest, IQPC15, consists of three tracks:

1. Evaluation of 2d footprints automatically generated from urban LIDAR data
2. Water detection and classification on multi-source remote sensing and terrain data
3. Tree Separation and Classification on MMS point clouds

This paper describes the set-up and the results of third track.

By visual inspection of MMS point clouds it is possible to identify separate trees manually, but this is obviously time consuming. The processing contest, therefore, addresses automation of this task. Two sub-tasks can be easily identified:

1. Classifying the points of an MMS pointcloud into two classes: tree points and other points
2. Separating the tree points in a point cloud into the individual trees

The emphasis in this contest is on separation. Therefore, the primary task for participants in the contest was to separate the trees in a given point cloud that contains only tree points.

In addition, participants were invited to analyse the raw MMS data, from which the tree points were extracted. The provided tree points only represent a subset of about 30 trees, but actually the number of trees in the area is much larger.

Therefore, participants who have access to classification software were challenged to identify as many tree points as possible, in addition to the ones provided, and after that separate the entire set of tree points into individual trees.

2.1 Available data

The MMS dataset is located at the campus of TU Delft in the Netherlands. It was obtained by the Fugro DRIVE-MAP system (Fig. 1). Fugro organizes the data in tiles of 25x25m. The raw

Figure 1: The Fugro Drive-Map system on the road

data consists of no less than 509 tiles, therefore occupying an area of about 318,000 m2. Note that many tiles contain only

very few points, and serve to fill up gaps between the other tiles (that do contain a lot of points). The total number of points is about 60 million.

Some 30 large trees were selected in a part of the area, which is contained in 26 tiles. There are some 10 million points in those 26 tiles, and the selected trees are made up of 1.8 million points.

We provide four datasets, each as a zip-archive containing files in the LAS Lidar format of ASPRS. The following fields are filled: X, Y, Z, R, G, B, i, t and c.

Here X, Y, Z are in Dutch RD/NAP coordinates, R, G, B represent a color as recorded by DRIVE-MAP camera's, i is the laser return intensity, t the GPS timestamp, and c a class label: 5 for tree points (high vegetation) and 1 for the other points (unclassified).
The following datasets were ready for download:

- alltrees.las.zip (21 MB): all tree points in a single file
- onlytrees.las.zip (21 MB): all tree points, organized in 26 tiles
- withtrees.las.zip (97 MB): 26 tiles containing tree points and unclassified points
- withouttrees.las.zip (429 MB): the remaining 509-26=483 tiles that have unclassified points only.

2.2 The Challenge

The challenge of the contest was:

- to subdivide dataset 1 or dataset 2 into as many groups as there are trees (approximately 30), and label the points accordingly.
- to classify (re-label) unclassified points in dataset 3, or in the combined datasets 3 and 4, as tree points where appropriate, and subdivide the entire set of tree points (the given ones and the newly classified ones) by labelling the points with unique tree numbers.

2.3 The Rules

The results may be represented either in LAS files or in ASCII files (with X,Y,Z and label on each line). When using LAS for challenge 1, the label can be stored in the so-called user field. This may give a complication, however, in challenge 2 if the number of trees is larger than 256. In that case an ASCII file is perhaps more suitable, but I am open to other solutions if clearly explained.

Results were to be submitted to the track organizer by 15th of June 2015 .

The evaluation of challenge 1 is quantitative on the basis of the number of correctly labeled trees, and qualitative, by visual inspection, on how well the points are assigned to the correct trees. The result gives the initial ranking of participants. In case of a draw, challenge 2 is considered. The criteria there are largely qualitive, by visual comparison of the results with the situation in the field.

3. THE RESPONSE

Results were received from three responders. Two of those produced classification as well as segmentation results, whereas the third addressed segmentation only. The descriptions of the different methods, along with illustrations, are included below and the respondents are among the authors of this paper.

3.1 Response 1

In this study an algorithm for efficient tree individualization and parameters abstraction from LiDAR point clouds is presented, as summarized in Fig. 2.

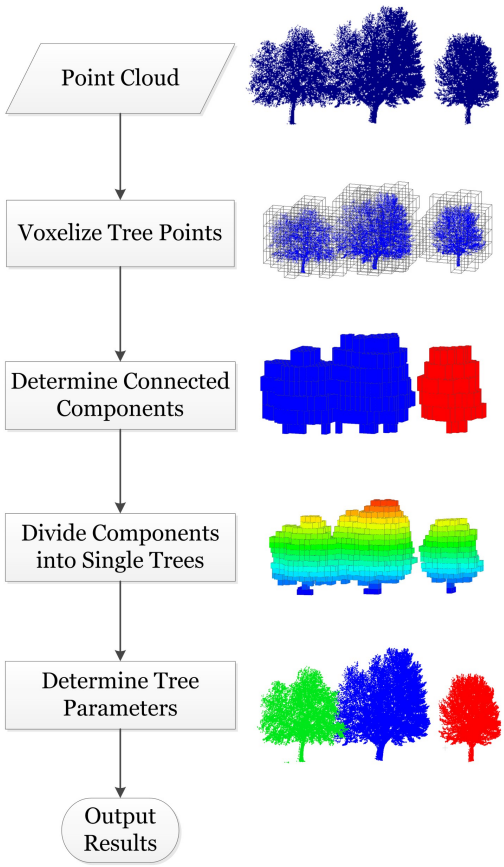

Figure 2: Segmentation Methodology in Response 1

The proposed algorithm takes the tree points as input and first resamples point data as voxel cells. Consecutively all the connected cells are clustered with a 3D seed filling algorithm

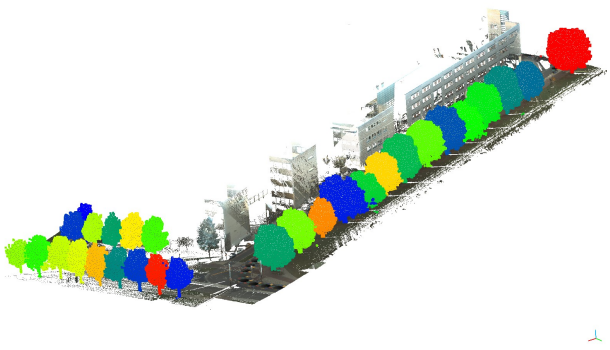

Figure 3: Tree segmentation with surroundings (response 1)

and the cells in multi-component clusters are further weighted with regard to connectivity factor of cells. Then by comparing the minimum distance between clusters with minimum tree diameter, touching trees are separated from top layer downwards. With the individualized tree points, typical

individual tree measurements such as location, height, volume, trunk length, canopy diameter, canopy height and basal area are determined. This algorithm is validated on airborne, mobile and terrestrial scanned point clouds of its efficiency and accuracy.

3.2 Reponse 2

In this study, we introduce a probability matrix computation based algorithm to classify and count individual trees in mobile laser scanning point clouds. Our method uses the 3D coordinates of the laser scanning points as input. At the first stage, it generates a new point cloud which holds a label for each point indicating if it belongs to the 'tree' or 'non-tree' class.

The classification is done by using a 2D probability matrix. The probability matrix is generated as a gridded plane on the x-y

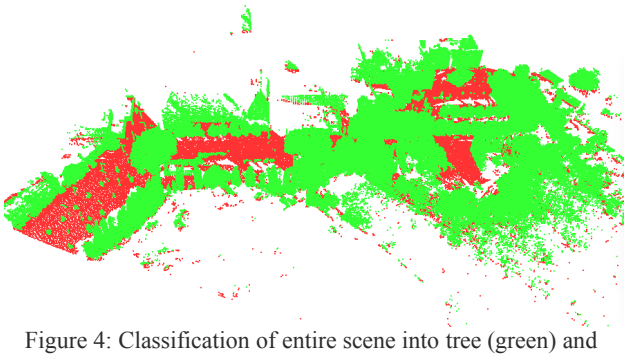

Figure 4: Classification of entire scene into tree (green) and other (red) points, in response 2.

plane of the input point cloud. Every grid cell holds the density of the point cloud within its boundaries. The probability matrix contains very high values at the tree trunk locations, but also at the locations of other vertical objects such as walls and light poles.

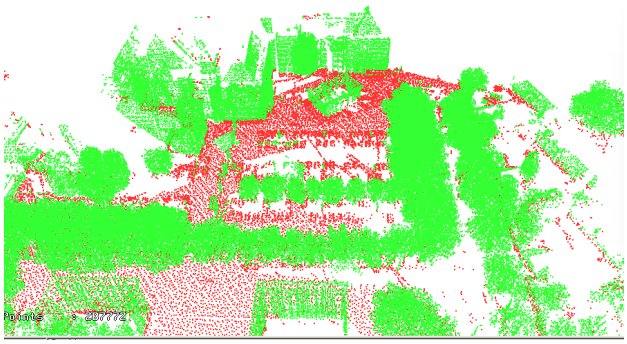

Figure 5: Classification of part of the scene into tree (green) and other (red) points, in response 2.

We apply local thresholding to extract high probability regions which could indicate trees. However after thresholding, we check the size of every segment in order to avoid false detection of walls. In this step, unfortunately false detection of pole like objects cannot be prevented.

The classification is done by assigning the value '1' ('tree' class) to the points which are close to the segments and the value '0' ('non-tree' class) to the rest. However some of the points receive '0' value even though if they are very close to a segment, when they are the lowest point in the neighbourhood or when the highest point in the neighbourhood is not higher than a tree height threshold (2 meters in our example). This condition is set for eliminating detection of the ground pixels under the trees and dense bushes which result having high probability values despite the fact that they are very low.

After assigning class labels to the input point cloud, we consider only the points which are labelled as trees and we separate individual trees using information accessed from the 2D probability matrix. To do so, we pick the local maxima of the 2D probability matrix and assume that they correspond to the positions of the tree trunks. We assign random ID numbers to the local maxima locations. Afterwards each point of the 'tree' class is assigned to the closest local maxima and gets its ID number as an attribute. As result, the new point cloud contains x,y,z coordinates and an ID number for each point. If the point cloud is visualized by false coloring according to the ID values, each individual tree appears in a different color.

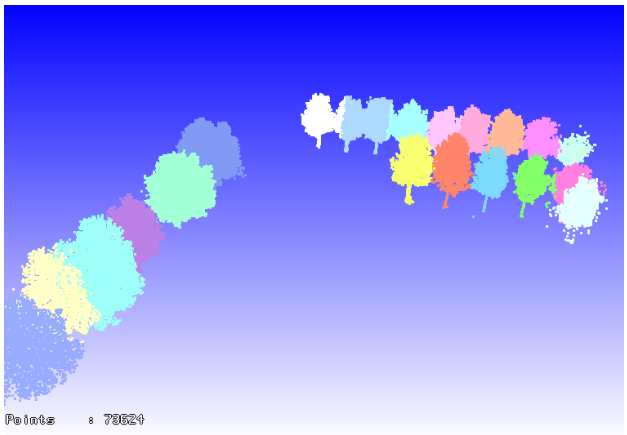

Figure 6: Segmentation in response 2

Our algorithm steps can be summarized as follows;

1- Generate a probability matrix
2- Select high probability regions from the probability matrix by local thresholding. If the areas are not larger than the given tree diameter size, assigning the closest points into the 'tree' class.
3- Selecting maxima of the probability matrix (which indicate possible positions of tree trunks) and giving a random ID number to each maxima position.
4- Generating a new point cloud for showing the individual trees. Picking each point from the 'tree' class and assigning the ID of the closest maxima as an attribute.

The algorithm works fast and gives reliable results even on point clouds of streets which contain many different objects. The experimental results indicate the possible usage of the algorithm as an important step for tree growth observation, tree counting, street monitoring, 3D city modelling and other similar applications.

3.3 Response 3

A way to detect trees in MLS data is shown step by step in the following sequence of figures. The input is a point cloud of only tree points, as provided by the track organizers. (Fig. 7). On this dataset, an initial connected component labelling is performed, with a radius of 1m, using 100 nearest neighbours in 3d (Fig. 8).

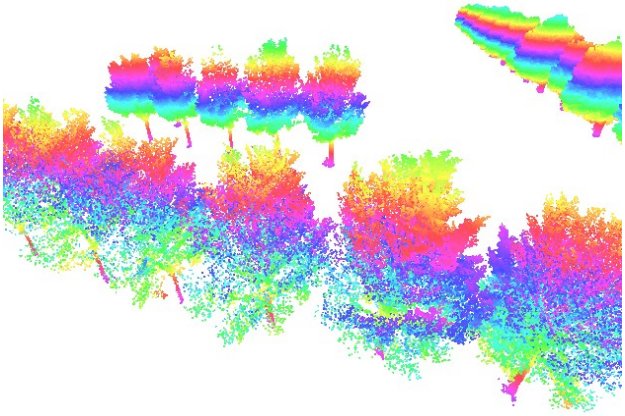

Fig 7: Input tree points, color coded according to height

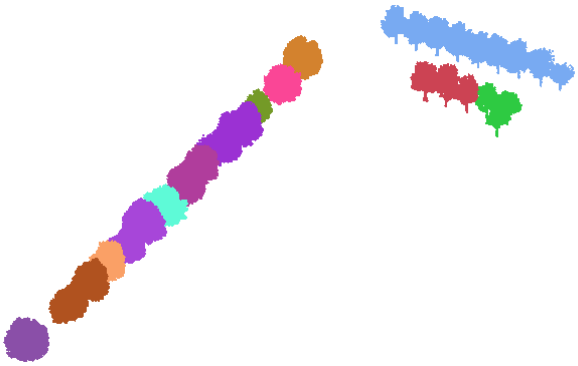

Figure 8: Result after connected component analysis:
13 connected components (response 3)

Where necessary the components are subdivided into individual trees by detecting whether at knee height (0.5-1 meter above the lowest point in the component) there are multiple segments [5].

Figure 9: Points labeled by height above lowest points.
Below 0.5 m (red), below 1 meter (green),
below 1.5 m (blue), others (yellow).

For components with multiple seeds at knee height we perform an upward & downward growing algorithm to try to assign the correct points to each of the growing seeds (Fig. 10). If within one iteration a point can be assigned to two or more segments, it is assigned to the one with the mean position closest to the point. For counting the number of trees, we do not need to assign all points to trees, we can just stop as soon as we have all the seed points at knee height. However, as we have to assign the points anyway, we just grow the seeds.

Some points have not been assigned yet, so a majority filter is applied. The result is in Fig. 11. Some more screen shots are shown in Fig. 12. Occasionally, points are incorrectly labelled, as shown in Fig. 13.

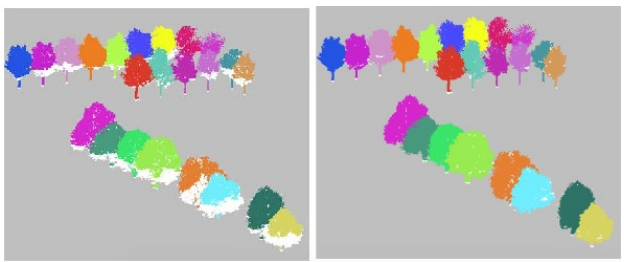

Figure 10: Components with multiple trees, after "upward growing" (left) and after "downward growing" (right).

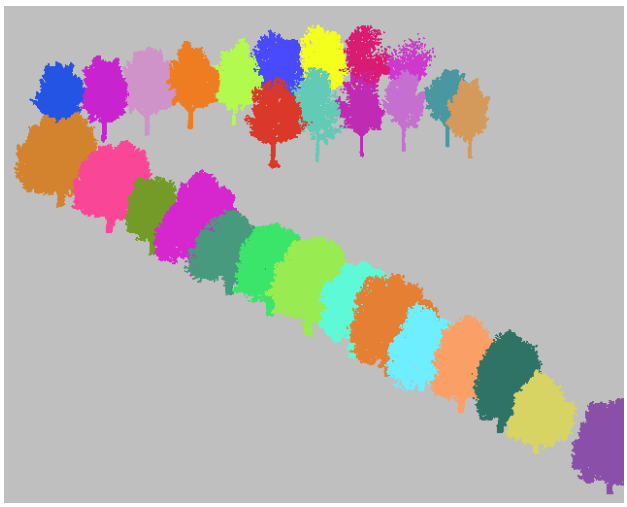

Figure 11: Segmentation result after majority filter (response 3)

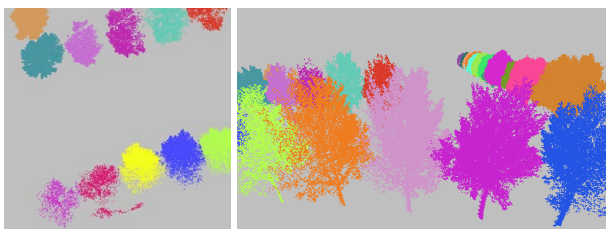

Figure 12: Segmentation details (response 3)

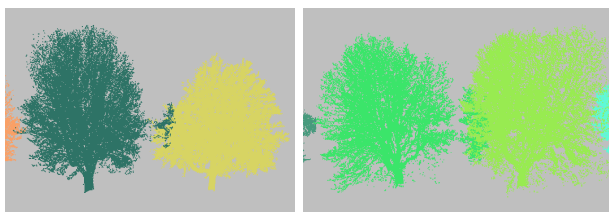

Fig. 13: Small segmentation errors (response 3)

For airborne laser datasets we have the option to detect local maxima and grow downwards from there. For MLS data is makes more sense to detect stems instead of tree tops.

Classification

The steps of the classification procedure of respondent 3 are as follows.

Step 1 consists of detecting ground segments. Attribute calculation, height above local lowest point (Fig. 14).

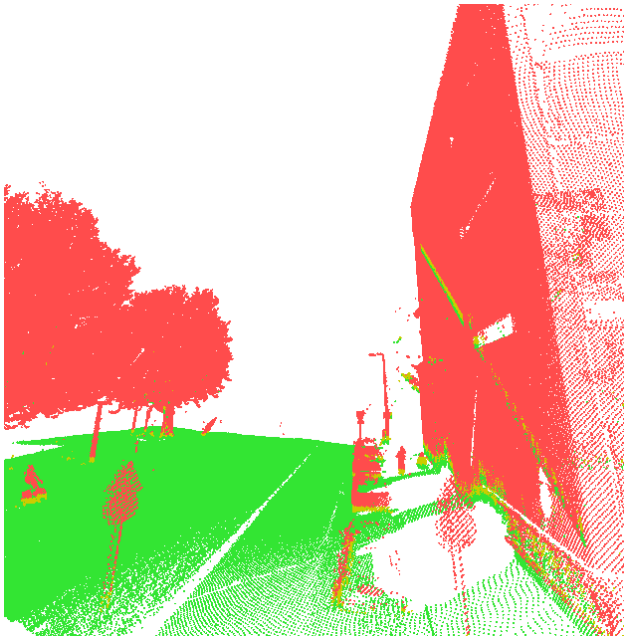

Figure 14: Ground points (green) and heights of other points (yellow and red)

In Step 2 the ground points (Fig. 15) are removed and the remaining points are submitted to constrained connected component labelling (Fig. 16). The constraint is that points are only grouped if their height above local lowest point is within 15 cm of the mean of the growing component.

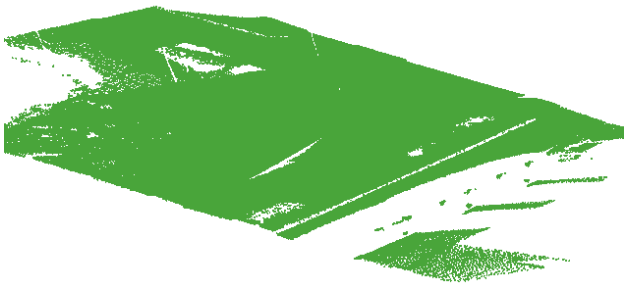

Figure 15: Ground points only

Next, it is checked which of the segments belong to the terrain (median value of all heights above local lowest points <15 cm).

Step 3 is separation of components with multiple parts at knee height (as explained in the segmentation section above). In this step individual trees, but also connected building elements, traffic signs, cars, etc. all get unique labels (Fig. 17 and 18, showing results at two different parts of the scene).

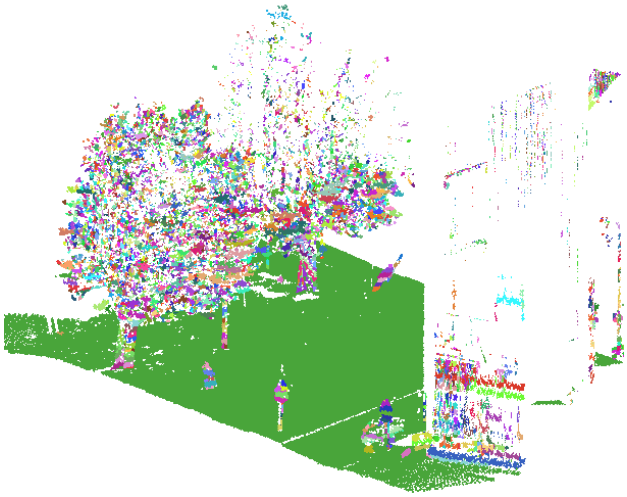

Figure 16: Constrained connected component labeling

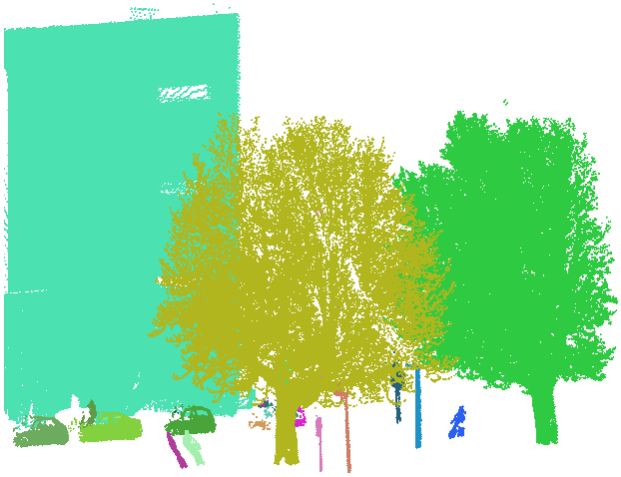

Fig 17. Final result after segmentation (response 3) (I)

Fig 18. Final result after segmentation (response 3) (II)

4. EVALUATION

Within the three responses that were obtained in this IQPC2015 track, the first was addressing tree segmentation only, whereas the second, in addition, considered classification of lidar points between trees and non-trees. The third respondent in fact provides a segmentation algorithm that separates a point cloud into all sorts of segments, including trees, without assigning class labels explicitly, however.

It is interesting to see that the three approaches to segmentation are entirely different, using a 3d grid (voxel) approach, a 2d grid (probability matrix) and 3d vector connected components, respectively. The grid approaches (both 2d and 3d) are apparently designed, at least partially, for the purpose of obtaining high processing speeds. Personal communication with the first two respondents revealed that they are working together in an attempt to process MMS *at 50 km/hour* (which has not yet been achieved, however). The third author reports much slower performances, but stresses that no attempts to optimization have been made yet.

It appears that using the voxel approach in response 1 good segmentation results can be achieved in the pre-classified (trees-only) dataset. An important difference between the approaches of 2 and 3 is the processing direction: top-down (literally, through the tree) vs. bottom-up. For respondent 3 this is a deliberate choice for MMS (as opposed to ALS), and it seems to be right: usually a tree has only one minimum (the trunk) at the bottom, but it may have several maxima (protruding branches) at the top, which would seem to subdivide the tree.

The grid-based classification approach looks promising, but thresholding does not yet sufficiently separate trees from other landscape elements having high 2d probabilities, such as lamp post and (sometimes) walls. The approach is currently being extended using 3d Principal Component Analysis (PCA) at high-probability grid cells.

The Constraint Connected Component Labelling approach (response 3) appears to provide superior segmentation results for different object classes simultaneously; however it does not distinguish between classes; therefore trees can only be counted in pre-classified tree-only datasets. Moreover, optimization is required before realistically sized datasets can be processed.

5. CONCLUSION

With three submissions the response to this track of IQPC15 was quite limited, and it might not provide a representative sample of the developments in the field.

However, the results shown are promising and it seems likely that they can be considered to represent the state-of-the-art in tree classification and separation. The diversity of approaches suggests that the field is still developing. One would expect to eventually arrive at a 'preferred' approach, perhaps depending on the input data (but the relation between the data and the approach would be clear). This stage has not yet been reached. Moreover, both the quality of the results and the speed of operation are still important concerns.

This track of IQPC15 was not fully executed: a performance test, by running the algorithms in a standardized computing environment, is missing. It would not have added much, as the three approaches are fundamentally different and partly not implemented with performance in mind. At a certain point in the developments the issue does become relevant, though.

Although perhaps to the disappointment of the reader, we are not ready to proclaim a winner amongst the three submissions.

ACKNOWLEDGEMENT

This research is partly funded by the FP7 project IQmulus (FP7-ICT-2011-318787) on the design and implementation of a high volume fusion and analysis platform for geospatial point clouds, coverages and volumetric data sets.

REFERENCES

[1] Hyyppä, Juha, Hannu Hyyppä, Paula Litkey, Xiaowei Yu, Henrik Haggrén, Petri Rönnholm, Ulla Pyysalo, Juho Pitkänen, and Matti Maltamo. "Algorithms and methods of airborne laser scanning for forest measurements." International Archives of Photogrammetry, Remote Sensing and Spatial Information Sciences 36, no. 8 (2004): 82-89.

[2] Kaartinen, H., Hyyppa, J., Kukko, A., Lehtomaki, M., Jaakkola, A., Vosselman, G., Oude Elberink, S.J., Rutzinger, M., Pu; Vaaja,N. (2013) Mobile mapping: road environment mapping using mobile laser scanning, European Spatial Data Research, Official Publication no. 62, pp. 49-95.

[3] B. Sirmacek, R. Lindenbergh, "Automatic classification of trees from LASER scanning point clouds", ISPRS GEOSPATIAL WEEK , France, 2015.

[4] B. Sirmacek, "Automatic Tree Detection from Laser Scanning Point Clouds", ISPRS GEOSPATIAL WEEK Silvilaser 2015, France, 2015.

[5] Oude Elberink, S.J. and Kemboi, B.J. (2014) User-assisted Object Detection by Segment Based Similarity Measures in Mobile Laser Scanner Data. In: ISPRS Technical Commission III / WG III/2 Symposium proceedings, 5-9 September, 2014, Zurich Switzerland. ISPRS Archives, Vol. XL-3. pp. 239-246.